UCRL-95593
PREPRINT

MULTILAYERS FOR X-RAY OPTICS

T. W. Barbee, Jr.

This paper was prepared for submittal to
Optical Engineering

May 20, 1986

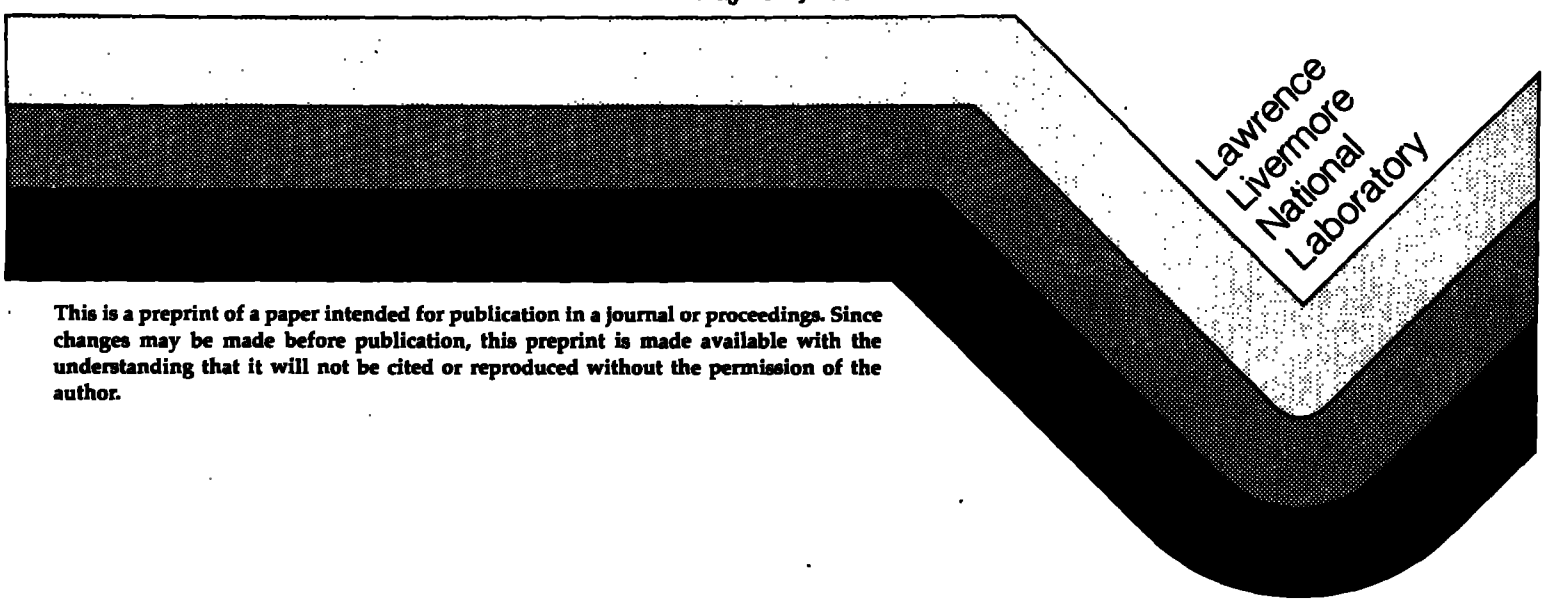

ABSTRACT

Soon after the discovery of x-rays and their property of constructive interference scattering (diffraction) by solids resulting from the ordered array of atoms forming the solids, it was proposed that man-made (synthetic) layered structures might extend the range of utility of this phenomena into spectral domains not accessible using naturally occurring crystalline materials. The synthesis of such layered materials has been of research interest since the 1920's and in the past decade processes for the formation of multilayer structures of quality sufficient for x-ray optic applications have been developed. In this paper a short review of the history of this work is given. The development of effective synthesis processes is then considered and current approaches summarized. The current status of the field of multilayer x-ray optics is then discussed with emphasis on figured structures. Current limitations and the potential for both technological and scientific advances are then considered.

Subject terms: X-ray optics; multilayer synthesis; multilayer properties

INTRODUCTION

The ability to manipulate x-rays in a useful manner using techniques applied in longer wavelength (lower energy) domains has been historically limited by both the basic physics of the interaction of condensed matter and x-rays, and by our inability to form stable microstructures of sufficient quality. During the past two decades significant advances in the sciences and the technologies important in the development of optics for x-rays have occurred, resulting in what has been termed a renaissance in this field. These areas are quite diverse and include: metrology at the angstrom level; formation of flat and figured surfaces having angstrom level uniformity; deposition of thin films uniform in thickness over large areas; deposition of these thin films in multilayer structures having thicknesses controlled so that all layers of a given material have the same thickness or known thickness; modeling procedures for flat and figured single surfaces and multilayer photon interactions; intense sources of extreme ultraviolet, soft x-ray and x-ray light (synchrotrons, pulse plasma,...) etc. It should be made clear that the needs of these new intense light sources have provided significant impetus for the development of experimental approaches resulting in the achievement of reproducible angstrom scale perfection, though general advances in many areas have yielded new capabilities pertinent to x-ray optics.

In this paper, a short historical review is given first. Multilayer synthesis processes are then considered and current approaches summarized. A general framework for consideration of multilayer structures on figured surfaces is then developed. A review of pertinent theory is then presented. Multilayers on figured surfaces are discussed at this point. Experimental results in this area are very limited so a more general discussion of the current status of multilayer development is included. A summary of the field is then given, opportunities for unique contributions being emphasized.

X-RAY OPTICS

X-ray optics as a field of investigation started at the turn of this century with the discovery of x-rays[1] in 1895. This was followed by the rapid application of classical techniques to the study of x-rays and the subsequent discovery[2] of the diffraction of x-rays by crystalline solids. These experi-

mental studies concluded that it was impossible to image, other than by simple projection, using x-rays. This resulted from the basic physics of the interaction of matter and x-rays.

The physics of this interaction is commonly described[2] in terms of the refraction index, $\hat{n}$, which is a function of the x-ray wavelength, λ, the elements comprising the body refracting the x-rays, and their concentration or number density. It is also important to note that x-rays are strongly absorbed by solids relative to the absorption exhibited by normal optical components. In general, the refractive index $\hat{n}$ is slightly less than 1 and complex, being given by:

$$\hat{n} = 1 - \delta - i\beta = 1 - (N_a r_e \lambda^2/2\pi)(f_{a1} + if_{a2}) \qquad (1)$$

where $N\hat{a}$ is the concentration of atoms a, r_e the classical radius of an electron, and λ the wavelength. f_{a1} and f_{a2} are wavelength dependent atomic parameters for species a directly related to δ and β which characterize the scattering and absorbing aspects of this interaction. The magnitude of δ is small, being for molybdenum, ~ 0.15 for 68eV light and $\sim 1.2 \times 10^{-5}$ for 10keV light. Therefore, $\hat{n}$ is nearly equal to but slightly less than unity. Coupled with the strong absorption, the small magnitude of the refraction coefficient precludes use of traditional transmission optics for the manipulation of x-rays.

It is in principle possible to construct reflecting optics, irrespective of the limitations of transmission optics. The efficiency of reflection is calculable[3] by means of the Fresnel equations. Since the refractive indices of solids are nearly equal to unity, the reflectivity at normal incidence is exceptionally small, being directly proportional to the square of the change in this index across a single interface. This is certainly the case, as observed by experimenters early in this century and more recently pointed out by Spiller[4]. At angles far from normal incidence (grazing), much higher reflectivity can be achieved.

In this domain, often termed total external reflection, light is specularly reflected if absorption is ignored. When absorption is included, a substantial

fraction is still reflected so that grazing incidence reflection optics may be constructed. The grazing angle θ_c, below which total external reflection occurs, is calculated using Snell's Law:

$$\text{Cos } \theta_c = \hat{n}_2/\hat{n}_1 (\simeq 1-\delta) \qquad (2)$$

where $\hat{n}_1$ and $\hat{n}_2$ are the indices of mediums 1 and 2: $\theta_c \simeq 0.29°$ grazing for 10keV light reflected from a molybdenum surface. It is important to note that this surface is assumed ideal, a concept discussed in more detail later. This has been used to design a wide range of reflecting grazing incidence imaging optics for x-rays, as well as optics for the manipulation of x-rays.

The design and imaging characteristics of such x-ray optic systems has developed into a discipline in its own right, influencing research in astronomy, laser fusion, magnetohydronamic fusion, plasma physics, and synchrotron radiation facilities as well as other areas. Such applications will be strongly affected by development of multilayer structures on flat and figured surfaces, particularly as non-grazing incidence systems can be developed. The construction of such optic systems will not be considered further here since I am primarily concerned with the reflecting surfaces and not their arrangements. Use of this literature will be made, though, in discussion of single surface reflectivity as this is of crucial importance for specular reflection and multilayer optics.

The effects caused by the magnitude of the refractive indices of solids for x-rays can, ignoring absorption, be overcome using multilayer structures in a manner directly analogous to the use of quarter wave stacks in standard optics,[3] or atomic planes in crystalline solids for diffractive optics.[2] At normal incidence, a quarter wave stack is identical to a crystal in that constructive interference of light scattered at the interfaces in the stack for a particular wavelength of light can result in high reflectivity. The actual path differences between scattering sites are optical path differences for quarter wave stacks and interplanar spacings for the diffracting crystal. Multilayer structures as described here lie between these two cases. An optics approach is therefore useful and will be taken in the following since refraction effects are

included. I also note that the optic approach treats the solid as a continuum while the diffraction approach includes the discrete atomic nature of solids.

The potential of multilayer structures was recognized soon after the discovery of x-ray diffraction by crystals when it was proposed that such synthetic materials would extend the range of this phenomena to longer wavelengths. Earliest attempts to synthesize multilayer materials failed primarily as a result of technological limitations. The first successful work reported appears to be that of Dumond and Youtz[5,6] who vapor deposited multilayers of gold and copper with periods of approximately 100 Å. These were found to be metallurgically unstable, the two components interdiffusing over a period of weeks. This field of research lay fallow until the 1960's when Dinklage and Frericks[7] and Dinklage[8] reported work on lead/magnesium, gold/magnesium, and iron/magnesium multilayer structures having periods of 30 to 50 Å. They observed degradation of the lead/magnesium and gold/magnesium structures while the iron/magnesium structures were stable for at least one year. These materials were tested with soft x-rays, the intended use being as dispersion elements in soft x-ray spectroscopy.

Other means for synthesizing multilayer structures using long-chain water insoluble fatty acid molecules were also developed in the 1930's by Langmuir and Blodgett.[9,10] This procedure has been refined and such structures are routinely applied as spectroscopic elements in the soft x-ray domain after adsorption onto flat and figured surfaces. Such molecular multilayers have been recently discussed[11,12] in some detail. Though these structures have significant scientific and technological impact, they will not be considered further here, as existing reviews provide a clear up-to-date description of this area.

At this same time initial efforts to utilize these layered materials for physical property studies was undertaken by Hilliard[13,14,15] and his students. This work represents the first direct application of multilayers as tools in materials research and yielded unique quantitative results on atomic motion in solids inhomogenous at the atomic level. The use of synthetic multilayer structures for physical property studies is an important developing area. It will not be considered further except in specific instances where results pertinent to the subject of this paper are used.

The field of multilayers for x-ray optics received new impetus with the proposal in 1972 by Spiller[4] that quarter wave stacks of scattering/absorbing materials could be effectively used as optics in the Extreme Ultra Violet (EUV) and low energy x-ray spectral domains with the specific goal of developing normal incidence imaging systems. He has used thermal source vapor deposition techniques to synthesize multilayer structures. Several other efforts were initiated during the mid-1970's. Schoenborn et al.[16] and Saxena and Schoenborn[17] initiated work on multilayer structures using thermal source deposition techniques for neutron optics and neutron polarizers. It is important to note that incoherent absorption can be minimized with neutrons so that very efficient structures are possible. Barbee and Keith[18] initiated work in 1976 on layered structures as a means for the control of the microstructure of thin films using sputter deposition techniques which has been extended to an extensive effort in multilayer x-ray optics.

As a result of this pioneering work, the field has expanded so that there are now many laboratories active in this area as well as two commercial enterprises. At this time there are significant efforts in France, England and the USSR, with efforts developing in Japan and The Netherlands. In the United States the developing work at the X-Ray Optics Institute at Lawrence Berkeley Laboratory, the University of Arizona, the Naval Research Laboratory, and the commercial activities of Energy Conversion Devices and Acton demonstrate the vitality of this developing research area.

The field of x-ray optics is clearly in the midst of a burst of activity which will result in new capabilities representing opportunities for the development of new technology and new science. This is clearly the result of the availability of high intensity light sources, the potential for new sources of even higher intensity and optic quality and the development of the ability to control microstructures both in depth and in plane resulting in whole new classes of x-ray optic elements which could only previously be imagined.

MULTILAYER SYNTHESIS[19]

Multilayer structures may be synthesized, in principle, using any technique in which the product is formed by means of "atom by atom" processes. Such techniques include physical vapor condensation,[20,21] chemical vapor

deposition,[22], electrochemical deposition,[23] and sequential absorption of insoluble monomolecular films suspended on a waterbath by substrate dipping. In this section, only "atom by atom" processes are considered, and then only those in which physical vapor condensation technology is used, a choice made since these processes dominate in reported experimental work.

Since the work of Dumond and Youtz,[5,6] many investigators have undertaken the synthesis of multilayer structures by means of physical vapor deposition for a wide variety of both scientific and technological purposes. Both thermal and sputter vapor deposition sources have been applied with success. Features both common and contrasting for these two types of sources will then be separately considered. Thermal source based technology is discussed first, followed by sputter source based technology. New approaches are then discussed.

Formation of a multilayer structure by physical vapor deposition requires the sequential deposition of two materials having the desired optical properties. There is, therefore, a common time sequence to the processes dictated by the structural parameters of the deposit and the synthesis technology used. Two specific procedures have been used. In one case the vapor beams are interrupted by shutters, and in the other the sample is moved through independent vapor beams in a controlled manner.

The time sequence is schematically shown in Figure 1 with $t = 0$ defined as the start of deposition of the first layer on the substrate. Negative time runs back through any "in situ" substrate processing, high vacuum pump down, roughing, to mounting of the substrate in the system. Positive time runs through the LSM deposition synthesis process, termination of layering, venting of the system, and removal of the substrate from the system. Although only the LSM deposition synthesis process is discussed in this section, it is important to understand that all these components are integral to the full synthesis process. Note that in Figure 1 time (Δt) when no deposition is occurring is shown and corresponds to a shuttering effect or to the rotation time between sources for a moving substrate case. This time segment is of potential importance since contamination of the multilayer from the system ambient can occur thereby affecting the multilayer quality and physical properties.

It is also important to note that in the static substrate-shuttered case the deposition rate for any given layer is essentially constant for the period

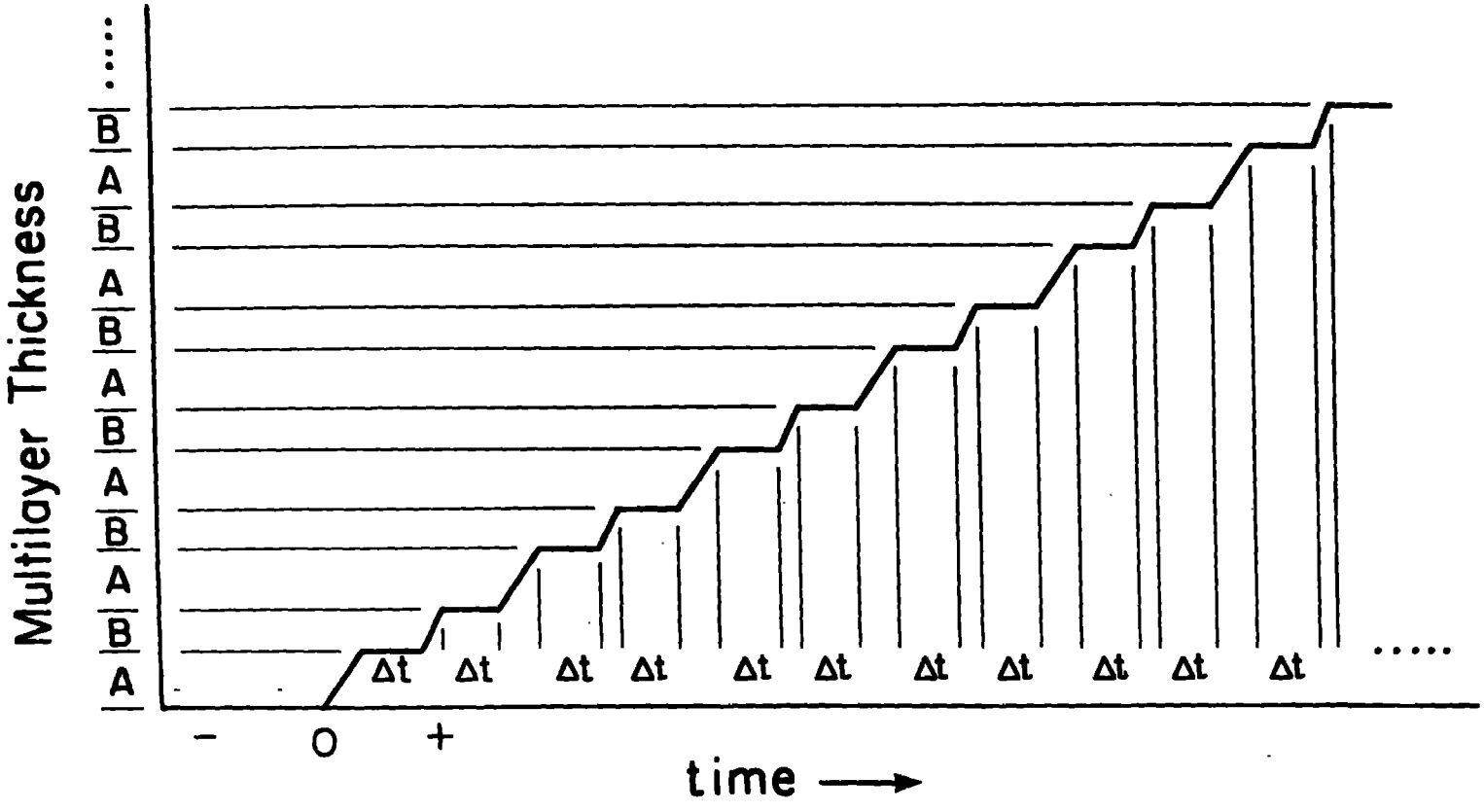

Figure 1. A schematic of the multilayer thickness-time relationship is shown. The time Δt is that between deposition of layers.

of deposition of the layer. In a rotating sample case the substrate sweeps by the deposition sources intercepting the sputtered or evaporated atom flux at a range of distances from and orientations relative to the sources. Therefore, the deposition rate varies in a monotonic fashion from zero to a maximum and back to zero as the substrate passes the source. The angle of incidence of the depositing atoms varies from value smaller than approximately 30° to the deposition surface at low deposition rates, to normal incidence at the highest deposition rates, and then back to low angles of incidence. This qualitative difference can affect the uniformity and structure of the layers deposited and should be clearly recognized.

Multi-vapor source configurations are used in the synthesis of multilayers with thermal sources. Typically, in these systems the sources and samples are stationary, the layering introduced through interruption of the vapor streams by shutters or by pulse timing in laser evaporation systems.[24] A schematic of a typical system[25,26] is shown in Figure 2. Sample sizes are usually less than 25 cm^2 but are dictated by specific system geometries.

In the application of thermal sources[21] the vapor pressure of the evaporant over itself is used as the vapor source. Energies of the evaporant are of the order of the source temperature, being almost always less than ~ 4000°K (~ 0.36eV). As the vapor pressure is strongly temperature dependent, tight control of the power applied to the source is necessary if constant deposition rates are to be maintained. Deposition rate control is accomplished using quartz crystal or ionization gauge rate monitors in a feedback control loop. These sensors continuously monitor the evaporating species and are arranged in a fixed geometry relative to the substrate surface and the vapor source. Deposition rates of from 2 to 100 Å/sec are typical necessitating feedback control time constants of fractions of a second. Additionally, the stability of the rate monitors must also be within the range sought; approximately $\pm$ 1 pct. Such stability can be achieved with quartz crystal monitors, though care to avoid thermally induced drift caused by radiation heating from hot evaporation sources is necessary, particularly with refractory metals.

The importance of deposition rate control other than for the obvious control of individual layer thickness is demonstrated in the work of Flevaris et al.[27] in which commensurate and incommensurate multilayer films of Cu-Ni were

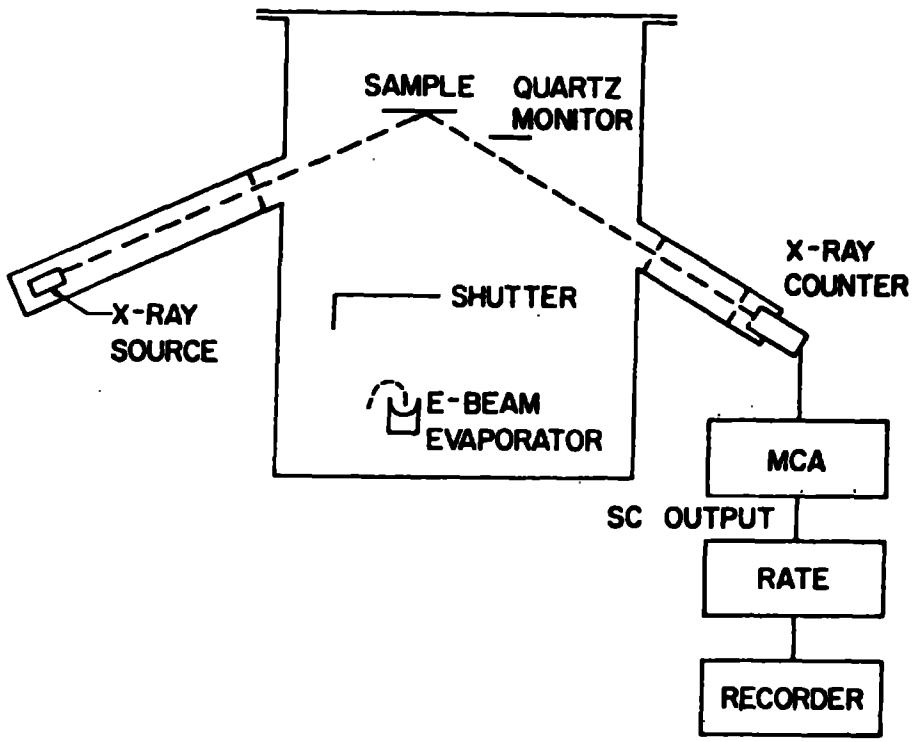

Figure 2. Schematic[25] of a thermal source deposition system with in situ monitoring of individual layer thickness. Electron beam sources are used.

synthesized and the character of the x-ray satellite peaks about the (111) crystal lattice reflection determined as shown in Figures 3a and 3b. The number of satellite peaks was observed to be a strong function of the commensuration of the multilayer structures. Structures which were nearly commensurate (i.e., integral numbers of atomic planes in both the nickel and copper component layers) exhibited up to six orders of x-ray satellite peaks. A comparison of the powder diffraction scan spectra obtained using Cu K_α radiation for two samples of essentially the same modulation period but varying in the degree of commensuration demonstrates this result. Therefore, high quality interfaces, in an x-ray sense, require that deposition rates be both well controlled ($\pm$ 1%) and well known in an absolute sense for high quality commensurate crystalline structures to be formed from dissimilar materials. This is undoubtedly the case for x-ray optic multilayer structures containing at least one component crystalline layer, incommensuration appearing as interfacial roughness or as a Debye-Waller type factor depending on the distribution of extra plane atoms on the interfaces.

A unique monitoring method used by Spiller[25] to fabricate multilayer soft x-ray mirrors was shown schematically in Figure 2. A soft x-ray reflectometer using characteristic line soft x-ray sources is installed in the evaporation system and continually monitors the reflectivity of a multilayer mirror during deposition allowing accurate control of the individual layer thicknesses (on the basis of property to be used) giving an experimental record of the x-ray optical thickness of each layer. This approach also allows characterization of the surface roughness of single films as a function of thickness, during synthesis. The reflectivity of a single film for monochromatic x-rays incident at a fixed angle, θ, is a function of the optical thickness of the film. This results from the interference of the x-rays scattered from the film-substrate and film-vacuum interfaces. If the film is smooth, the reflectivity will oscillate about a constant value, the amplitude of the oscillations decreasing with increasing thickness due to absorption in the film. If the film roughens with thickness, the reflectivity oscillates about an average value of reflectivity which decreases with increasing thickness. An example[25] is shown in Figure 4 for AuPd deposited by thermal evaporation onto a silicon substrate with the roughness, σ, derived by use of the Total Integrated Scatter formalism discussed

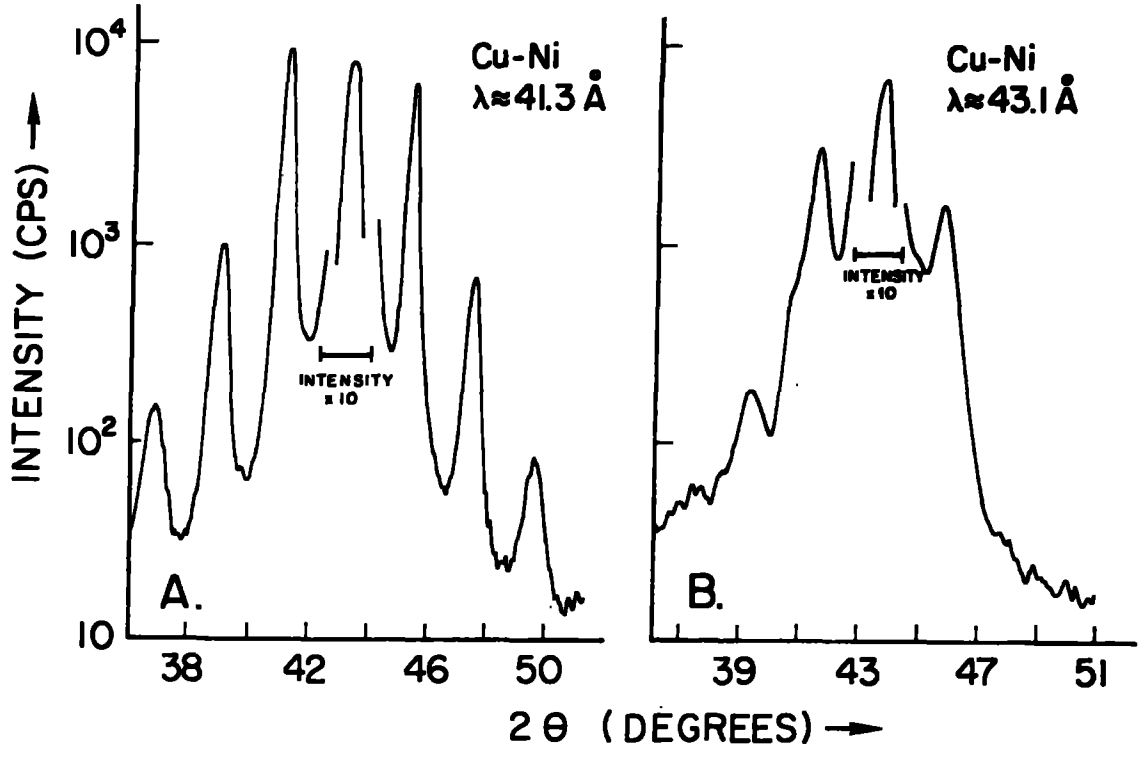

Figure 3. Powder diffraction scans[27] from two samples of composition modulated Cu-Ni. The difference in sideband definition indicates that one sample is commensurate (3A) and the other incommensurate (3B).

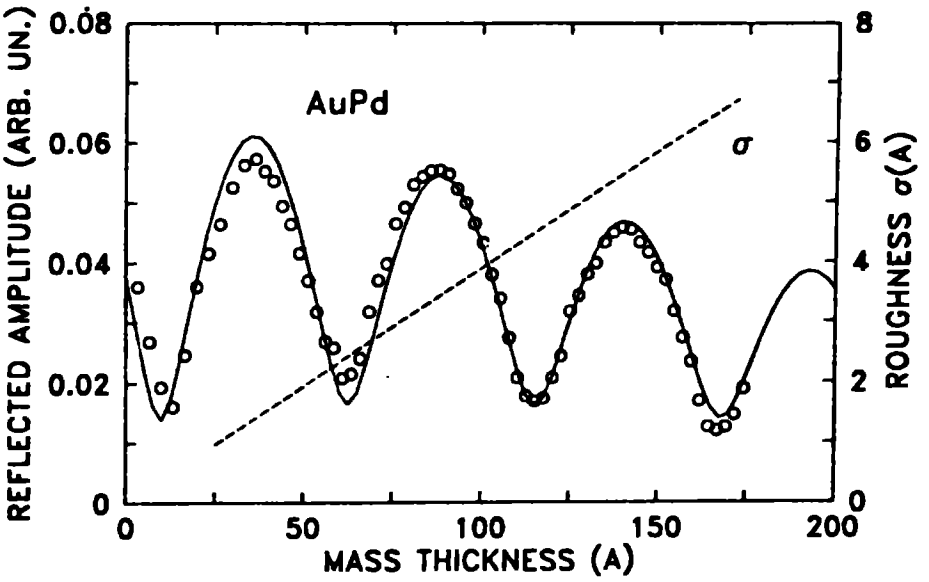

Figure 4. Thickness dependence of the measured[25] reflected amplitude for AuPd on silicon for λ = 44.7 Å and α = 64° shown with a theoretical curve calculated assuming the surface roughness indicated.

later in this paper. Increased film roughness with increased thickness is not always observed. In some cases, when a film is synthesized by deposition of many thinner layers, or when a multilayer is synthesized, decreased roughness or smoothening is observed as the deposit thickness increases.

Thermal sources may be classified as to whether crucibles are required. Crucibles are most often needed when resistive heating is used. Due to the thermal mass typical of such resistively heated sources, the time constant of the feedback control loop is determined by the thermal time constant of the crucible/molten evaporant body. It is likely that the deposition rate control level will not exceed $\pm$ 5% with such systems. Crucibleless sources typically depend on skull melting (i.e., containment of the molten bath in a solid shell of the same composition) as is characteristic of electron beam heated sources and "pulse" laser vapor sources. Heating with electron beam sources allows time constants of the order of 1 sec to be attained. In the case of pulse laser sources, a solid surface is illuminated with a short high energy density laser pulse. Control of the deposited energy results in control of the volume of material evaporated. Therefore, in principle, if the deposit is monitored, a very short time constant can be approximated. Crucibleless sources are preferred as a result of the enhanced control as well as the elimination of the possible contamination of the evaporant by the crucible material.

Thermal sources also exhibit characteristic deposition profiles, i.e. substrates normal to a vector normal to the bath surface are not uniformly deposited upon at all positions. The effect of the nonuniformity can usually be minimized by placing the substrates sufficiently far from the evaporation source or by moving the substrates so that all regions of experimental interest intercept the same time integrated flux of evaporant for a given layer. Substrate motion is only necessary when large areas are needed or when specially formed substrates are used, as might be required by x-ray optic applications.

The energy of the evaporant atoms is generally less than $\sim$ 0.4eV and any gas scattering may markedly affect the deposition process. Therefore, vacuum requirements are for pressures allowing "line of sight" paths for the evaporant atoms, source to substrate; required pressures are always smaller than $\sim 10^{-4}$ Torr. A more restrictive boundary condition is that necessary to minimize contamination of the depositing material by reactive components in the ambient

atmosphere of the vacuum chamber. The kinetic theory of gases indicates that at a pressure of $\sim 5 \times 10^{-7}$ Torr a sufficient number of atoms (if condensed) to form a monolayer impinge on the substrate per second. Therefore, if the constituents of the evaporator ambient are reactive with the depositing materials, significant contamination can occur which may degrade the structural and physical characteristics of the deposited multilayer.

Process limitations inherent to thermal source synthesis of metal multilayer structures include deposition rate control, contamination of the depositing film by ambient vacuum constituents, and limited sample area. Other limitations result from radiation heating of the substrates during deposition and from fractionation of alloy charges during evaporation. Radiation heating, particularly when high melting temperature elements are being deposited, makes substrate temperature control difficult, but with feedback and a low thermal mass for the heater/substrate body, engineerable. Fractionation of alloy melts as a result of widely differing vapor pressures precludes single source deposition of many alloys and compounds. In more general deposition experiments this is overcome by use of a single vapor source for each component of the alloy which requires accurate deposition rate control to maintain stoichometry and many sources if alloys of order higher than binary are to be condensed. Hence, quite complex systems can be envisioned for synthesis of multicomponent metal multilayer samples.

Multisource configurations are also used in sputter deposition systems[28,29] designed for multilayer synthesis. In these systems the sputter sources are widely separated and the substrates moved past the sources, a single layer being deposited on each pass by a source. A schematic of such a system is shown in Figure 5. In work performed using such systems, traditional glow discharge sources and more advanced sources such as magnetron and triode have been applied. Sputter sources use solid targets and can be operated in the deposition up, deposition down, or horizontal deposition modes facilitating coating of nonuniformly configured surfaces as well as very large surface areas.

Sputter sources are solid materials, atoms or atom clusters being ejected from the solid target into the vapor by bombardment of the target surface with energetic particles. The ejected atoms impinge on a substrate condensing to form a film. In most cases noble gases are used as the sputter gas, their ions

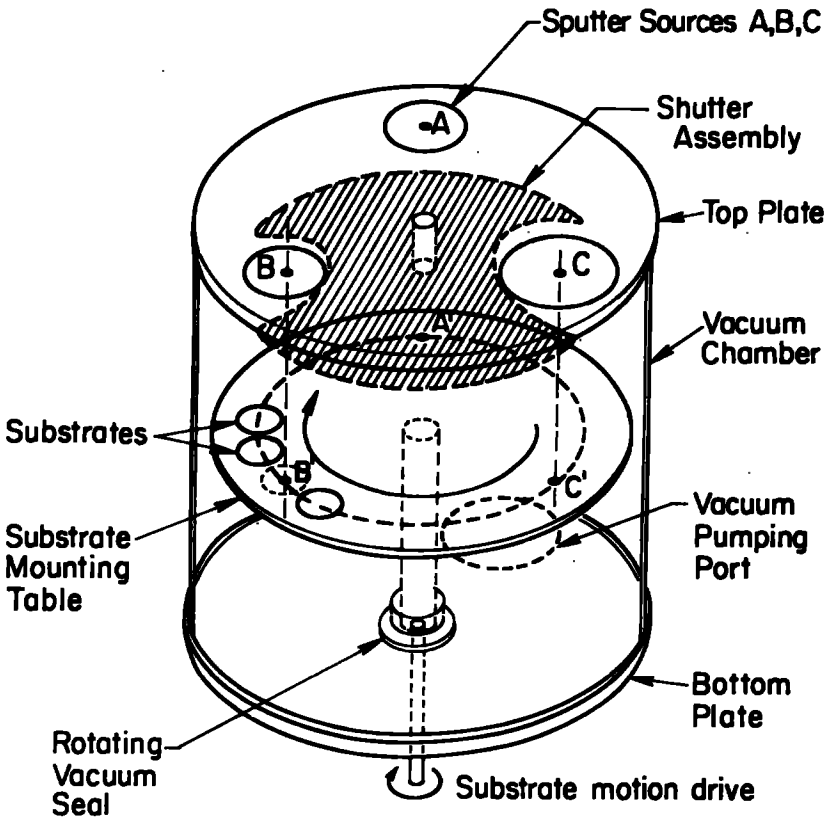

Figure 5. Schematic diagram of a typical multi-source sputtering system used to deposit superlattice films. A, B and C are sputter source positions. Substrates are mounted on a rotating table, a layer being deposited as the substrates pass by each source. The individual layer thicknesses are determined by the deposition rate of the sputtered material, the rotation speed of the table, and the source to substrate spacing.

being thus positively charged: the process is called cathodic sputtering. Ions are formed by establishing a plasma in much the same manner as a glow discharge is formed in a low pressure gas by an electric field between two electrodes. In the past two decades several advances in sputter source technology have occurred. In these new approaches, increases in the efficiency of secondary electrons in ionizing the inert gases by means of magnetic field structures (magnetron sources), increasing the availability of electrons for ionization (triode sputter sources) and independent ion beam sources have been developed. The advent of these new sources has allowed the technology of sputter deposition to advance in a rapid manner so that significant increases in deposition rate and deposit purity have been attained. In the following, a short discussion of the important features of sputter deposition sources[20,28A] relative to multilayer synthesis is presented. The factors to be considered include sputter source-deposition surface coupling, energy distribution of the sputtered atoms, and the geometry of the vapor source--substrate configuration.

The sputtering process entails establishing a plasma discharge and imposing a potential of the correct polarity so that ionized gas atoms are accelerated to the cathode surface where, if of sufficient energy, they dislodge other atoms. These secondary atoms travel from the cathode surface to the deposition surface, being adsorbed to form a deposit. Other types of primary sources exist in which a plasma of the species is generated and accelerated to the deposition surface. Therefore, all such sources are plasma based and source-deposition coupling can be characterized by the degree of plasma-deposition surface interaction.

During the past decade new sputter deposition sources have become available in addition to the conventional diodes. All these can be operated in both DC and RF modes, the nature of the particular application and material to be deposited dictating the mode of excitation. The "new" sources include triode supported plasma sources, magnetron sources and ion beam sources. A common characteristic of these new approaches is that high deposition rates (approximately an order of magnitude) larger than possible with conventional diodes are observed. In addition, control of the plasma characteristics and the deposition surface environment are possible with these new devices.

The mechanisms of plasma coupling include[20] secondary electron bombardment, inert gas ion bombardment, neutral inert gas atom bombardment, and vacuum

ultraviolet irradiation. In conventional diode sputtering it is estimated that 10% of the cathode power is deposited at the substrate in RF deposition and 30% for DC sputtering. In both cases it is clear that more than half of this is due to secondary electron bombardment. The distribution of energy among the other factors is less well defined. The primary result of secondary electron bombardment is substrate heating and, in the case of semiconductors or insulators, electronic defects.

Bombardment by either neutral or ionized inert gas ions results in heating of the substrate and enhanced atomic mobility for depositing atoms at the sample surface. It is also possible to induce ion implantation resulting in a high concentration of inert gas being entrapped in the deposit. In addition, the ion bombardment will result in mixing at the deposit surface which may be one or two nanometers in extent, degrading interface character.

Magnetron sources, in which a magnetic structure behind the target surface provides a magnetic trap for the secondary electrons active in the plasma ionization process, exhibit deposition rates a factor of 10 larger than those characteristic of conventional diodes. The magnetic structure provides a field normal to the electric field of the source diode which results in a closed toroidal trajectory for the electrons. Such secondary electron trapping allows isolation of the sample from the secondary electrons. In addition, the magnetic structure clamps the plasma at the cathode surface so that the sample can be isolated from bombardment by charged particles. Control of neutral particle bombardment is not typically considered significant, but is not well understood. It may be quite large as reflection coefficients are considered large for backscattering of low energy atoms characteristic of plasmas in magnetron systems. In addition, bombardment of the cathode target surface can result in implantation of inert sputtering gas ions so that the target material becomes an alloy, one component being the inert gas.

It is extremely difficult to decouple the sample from the plasma with conventional diode sources. By way of contrast, it is in principle possible to fully decouple[20] (except for U.V. radiation) the plasma from the substrate when magnetron sources are used. This results in a degree of synthesis process control and of purity heretofore not possible with sputtering.

The effects of this sputter plasma-deposition surface coupling[30] is shown for traditional glow discharge diode sources in Figure 6. In this figure the amplitude of composition modulation determined by x-ray diffraction analysis is plotted as a function of individual layer thickness for InSb/GaSb multilayers sputtered at argon pressures of 1, 3 and 15 m Torr. Layer thicknesses in each sample were equal to half the modulation wavelength. The increase in argon pressure acts to thermalize the sputtered atoms by gas scattering and reduce substrate bombardment by the same mechanism. The important point is that for fixed layer thickness the composition modulation increases as the argon pressure increases and the degree of ion bombardment decreases. Ion bombardment during synthesis provides knock on mixing between layers. Therefore, compositionally abrupt interfaces cannot be synthesized using traditional sources as a result of such sputter plasma-deposition surface interactions.

Compositionally abrupt interfaces can be formed if magnetron or other ion beam sputter deposition sources are used. In such cases it is experimentally possible to isolate the deposition surface so that backscattered argon is the only plasma generated specie other than the depositing specie incident onto the substrate. Under these conditions the kinetic energy of depositing species is the major contributing external energy source.

The kinetic energy distribution of atoms ejected from the cathode by the incident high energy ionized inert gas atom bombardment is dependent on the angle of incidence of the sputter gas ion onto the cathode, the mass ratio of the sputtered atom and the sputter gas, the sublimation energy of the cathode material and the energy of the incident sputter gas atom. Gold sputtered using 600eV argon atoms at normal incidence has an mean energy of approximately 13eV with a high energy tail extending to 50-80eV. This adds substantial energy to the deposition surface[31] and can cause high bulk substrate deposition temperatures at moderate deposition rates. For example, if gold, sputtered with 1 keV argon, is deposited at a rate of 1000 Å/min, the deposited power flux is 0.021 watts/cm^2. This power is directly coupled into the deposition surface which is no more than a few angstroms thick resulting in a very large deposition rate of power per unit volume ($\sim 10^5$ watts/cm^3 sec) for the sample surface region. It also causes a substantial increase in the bulk substrate temperature for thermally isolated substrates; 180°C with low emissivity and 50°C with high

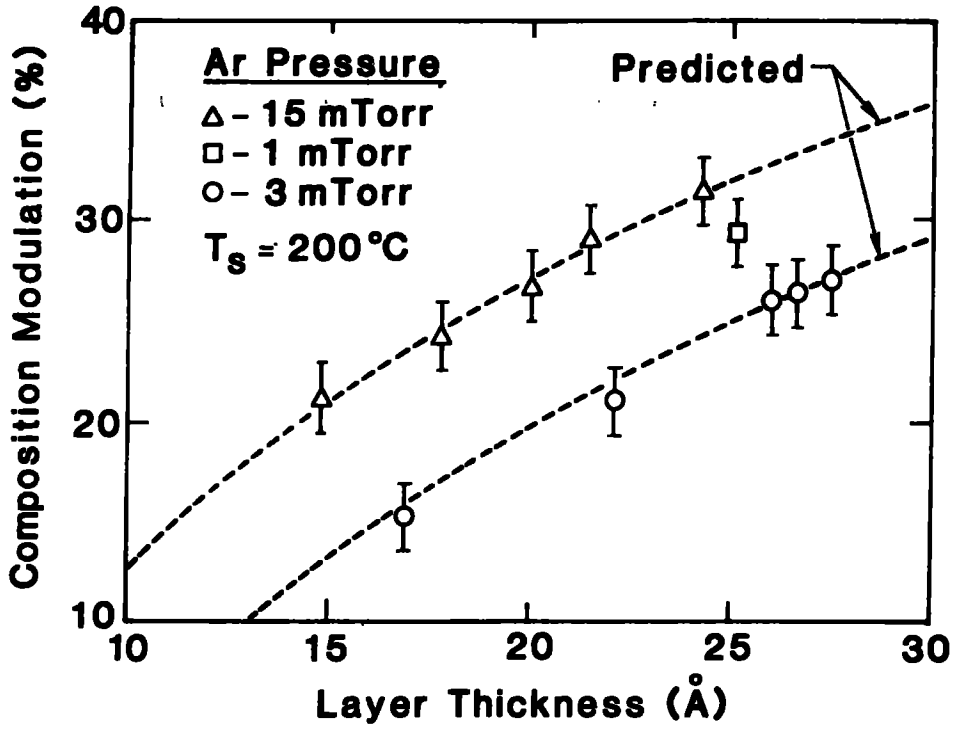

Figure 6. The amplitude of composition modulation in InSb/GaSb superlattice films grown at 200°C at different Argon sputtering gas pressures using traditional diode sources as a function of layer thickness.[30]

emissivity. The effects of this energy deposition at the deposition surface are not well understood. It has been verified though that bulk substrate heating effects in accord with calculation are observed. Also, the sputtered adatoms can be thermalized by gas scattering by operating at high inert gas pressures (30 m torr) minimizing this effect.

The geometrical arrangement of the sources and substrates is important as this defines the angle of incidence of the depositing specie onto the substrate. In standard deposition experiments the sample is fixed relative to the source, deposition occurring by line of sight motion of the sputtered species from the target to the substrate. If the substrate is "ideally" smooth and clustering can be ignored, the deposited film will, in thickness, exactly replicate the deposition profile of the source at all positions. If the substrate is rough on a near atomic level (5 to 50 Å lateral period) the solid angle subtended by a unit area of substrate will vary with position on the substrate and hence the local deposition rate will spatially vary. This is an unstable growth condition and results in substantial roughness as well as non-uniform layer formation. Such substrate roughness will also strongly influence the inplane or lateral crystalline coherence of the deposited films. If nucleation occurs on each facet of the rough substrate surface and growth is with the close packed plane in the plane of deposition, the lateral coherence of crystalline films will most likely reflect the scale of the surface roughness. This places very high requirements on substrate quality relative to surface roughness since with multilayer films the scale of the layering is typically of the order of 10 to 1000 Å.

In the case of sputter deposition these effects are moderated by the motion of the substrates past the sputter sources. Sputter sources are distributed in nature providing deposition at many angles of incidence at the substrate. Additionally, the motion of the substrates past the source results in deposition at nearly all angles of incidence. These two effects minimize the role of substrate roughness in producing films of non-uniform thickness but will have negligible effect on the lateral coherence degradation by substrate roughness.

Although the multilayer quality achieved using existing technology is excellent in many cases, the need for enhanced control during synthesis by means of "in situ" monitoring and for new approaches having unique characteristics,

possibly specific to particular materials, is clear. Efforts in such areas are now coming to fruition and include ion beam sputter deposition, "in situ" monitoring using elipsometry, and plasma-assisted chemical vapor deposition among others.

In ion beam deposition[20] a low energy plasma, contained in an ion gun chamber, provides ionized atoms which are accelerated by means of a grid system to the desired energy. This ion beam impinges onto a target, ejecting atoms which condense on a substrate to form a film. The important characteristics of this approach are that the plasma is isolated from the deposition surface and the gas supply required is substantially reduced as the active plasma volume is within the gun housing. Therefore, control of the environment at the deposition surface is strongly enhanced. In particular, only back scattered neutral sputter gas atoms and condensing atoms impinge on the substrate. Also, it is possible to maintain pressures at the substrate which are two orders of magnitude smaller than with magnetron sputtering systems. Although deposition rates are substantially smaller than with magnetron sputtering, the enhanced control and cleanliness are important advantages.

Ellipsometric monitoring of multilayer synthesis[32,33] is being pursued by laboratories in France, Japan and the United States. Such systems have the advantage of using visible light and well-known technologies. It appears at this point that thickness sensitivities for dense elements will be below 1 Å. Sensitivities for lighter elements are of the same order but not quantitatively characterized at this time. Though "precision" ellipsometry is required, effective monitoring can be carried out using commercially available instrumentation.

A more generic advance has been made by Abeles and Tiedje[34] who reported synthesis of multilayers by a plasma-assisted chemical vapor deposition process. The materials were hydrogenated films of amorphous silicon, amorphous germanium, amorphous SiN_x, and amorphous $Si_{1-x}C_x$. Layering is achieved by periodically changing the gas in the plasma reactor without interrupting the plasma. Growth rates were approximately 40 Å/min. The gas exchange time for the reactor was 1 sec so that only a fraction of a monolayer was deposited during gas changes. Multilayers having individual layer thicknesses of $\sim$ 1.3 nm and interfacial roughness of < 5 Å have been synthesized. Though the

materials used in this work may not be of use in x-ray optics, the process is promising since it is likely that very thick deposits which contain many thousands of layers may be synthesized as a result of the continuous nature of this process.

SCHEMATIC MODEL

An effective framework for the discussion of multilayers on figured substrates can be developed by systematic construction of a hypothetical multilayer. It is then possible to define the range of structural and physical characteristics of each component, specific combinations of components, and the full multilayer structure. A schematic diagram in which the substrate, component layers A and B, interfaces between the substrate and layers A or B, interfaces between layers A and B, interfaces of layers A or B with ambient, and the full multilayer structure are outlined is given in Figure 7. Implicit in this approach is a temporal scale with time equal zero at the substrate, increasing as the multilayer is synthesized in a manner consistent with the synthesis processes previously described.

Included in Figure 7 is a listing of statements and questions defining important characteristics of the components of a multilayer. Most of these terms are self-explanatory, while others require explanation. First, there has been a separation of surface structural quality into two domains: that in which geometric scattering is controlling, and that in which diffractive scattering is controlling. The ideal case for the geometric domain is termed <u>flat</u> and includes figured surfaces where deviations from the desired figure have geometric effects. The non-ideal case is termed <u>unflat</u>. The ideal diffractive case is termed <u>smooth</u> and the non-ideal case <u>rough</u>. These domains are typically differentiated by the scale of the surface structure, both in plane and normal to the mean surface plane. The terms <u>clean</u> and <u>contaminated</u> indicate the presence of undesired and often uncontrollable species on the deposition surface starting with the substrate. Note the deposition surface is present during the full synthesis process. Such contaminents may therefore be included in the depositing layers, or, as a result of the time sequence of layering, be more concentrated at the interfaces between layers.

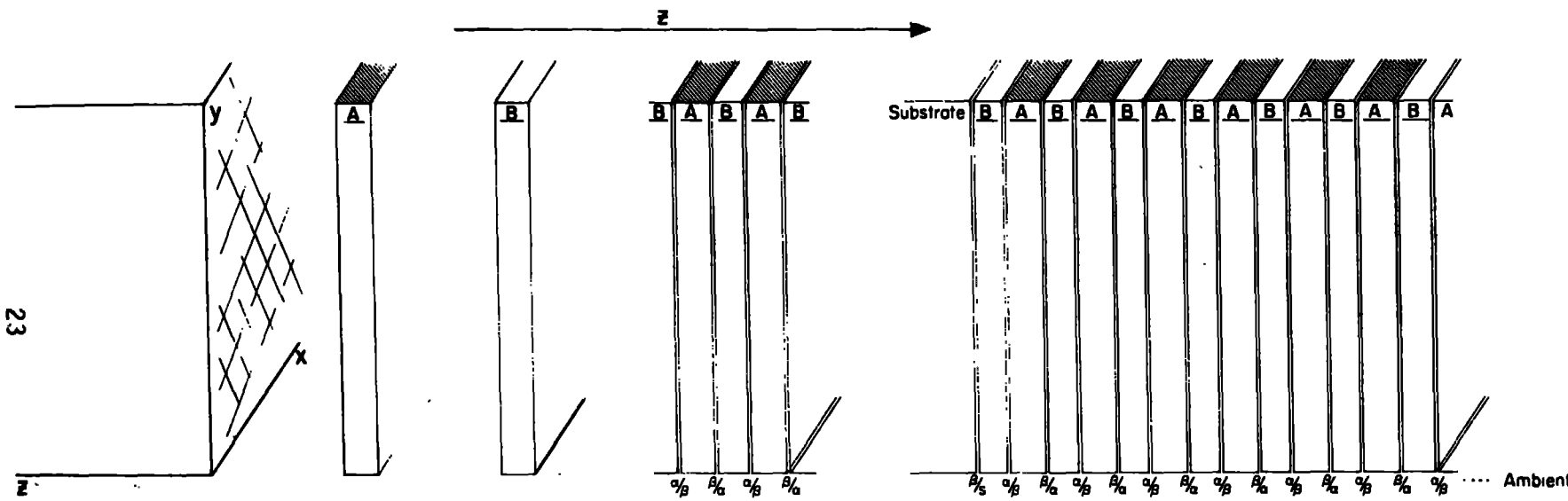

Figure 7. The components comprising a multilayer film are schematically shown. Pertinent questions concerning these components and their interrelationships are listed.

The individual layers have a specific set of properties directly related to bulk forms of the particular materials (A and B). The primary questions are: what are the compositions and the structures of the layers; do the optical properties of the layers correspond to bulk properties; and is the number density of atoms in a given layer per unit surface area the same for all unit areas or in accord with multilayer design? The range of unit area starts at the level of the effective surface area of single atoms increasing to the full area/scale of the multilayer. The concept of areal atomic concentration in a layer is one way to formally describe non-uniform thickness independent of roughness or flatness. Specific synthesis questions relate to the film nucleation and growth behavior as deposition of material A onto a substrate or layer B may differ substantially from deposition of B on a substrate or on layer A.

Interfaces within the multilayer have these same characteristics (flat, unflat, smooth, rough, clean, contaminated) with the additional characteristic that they may be compositionally abrupt or compositionally graded over some distance in the growth direction. Compositionally abrupt means that composition changes, A to B, occur over one atomic distance normal to the interface. Such abruptness does not preclude roughness though it may be experimentally difficult to differentiate rough compositionally abrupt from compositionally graded interfaces (rough or smooth). Interfaces are specifically described as layer A onto the substrate or to ambient (α/S or α/A respectively), layer B onto the substrate or to ambient (β/S or β/A respectively), layer B onto layer A (β/A) and layer A onto layer B (α/β). This level of detail is used as the equivalencies of α/S to β/S, α/A to β/A, or β/α to α/β are not known.

Multilayer structures themselves represent a composite of all the specific characteristics of the individual component elements. It is in principle possible to describe the structure of a multilayer by specifying each of the particular features as previously delineated for each appropriate position in the structure. Since this is not easily done, the approach of preference will entail statistical averages over the structure as a whole. Such averages will be correlatable with experimental reflectivity data, optic quality data, image quality, focal spot size for focusing structures, etc., as the observed

responses average over the structure active in the specific characterization measurement. Additionally, since the observed responses cannot be, in most cases, unambiguously traced to a specific structural feature of a multilayer, care must be exercised when interpreting experimental results.

As a case in point, measured reflectivities are typically not of the same magnitude as those predicted. This has been rationalized as resulting from interfacial roughness between layers, but could also result from compositionally graded interfaces, scatter of the period of the multilayer about some averaged value, unflat substrates causing light to be scattered out of the aperture of the detector, use of incorrect optical constants in the modeling calculations, etc. Therefore, rather more detailed measurements than have been typically performed up to this time, as well as experiments using samples into which known defect structures have been included, are needed so that specific correlations may be realized.

THEORETICAL BACKGROUND

The theoretical background for this paper includes three major subjects. The first is concerned with x-ray scattering by single surfaces of semi-infinite solids. The second is scattering by a composite structure consisting of thin films deposited on such surfaces. The third is scattering by multilayer structures deposited onto such surfaces. Only a brief outline of these areas is given as background.

X-ray scattering from single surfaces, when considered in detail,[35,36,37] is a complicated process. It has to this point been treated in a continuum framework by means of the Fresnel equations, with little effort to include the atomic nature of solids. Therefore, the continuum approach will be emphasized here. The Fresnel equations apply specifically for plane waves incident onto a planar boundary. It is important to understand that the Fresnel equations calculate the magnitude of specularly reflected light; the scattering angle is equal to the angle of incidence. No provision for non-specular scattering is included. Surface planarity in this situation has a specific relationship to the wavelength of the incident light; the radius of curvature of the scattering surface should be much larger than the wavelength of the reflected light. This is thought to be met in the x-ray domain but may be problematic for soft x-rays

or EUV light. In particular, surfaces of real solids, even if "atomically" smooth, have a roughness dictated by the discrete nature of atoms. Such atomically smooth surfaces are experimentally rare, so that microscopic roughness must be considered and is discussed later.

The Fresnel equations give the reflected amplitude[3] at the boundary of two materials of complex refractive indices $\hat{n}_1$ and $\hat{n}_2$. The amplitudes of reflection of σ(S) and π(P) polarized light are:

$$r_s = \frac{\hat{n}_1 \cos \alpha_1 - \hat{n}_2 \cos \alpha_2}{\hat{n}_1 \cos \alpha_1 + \hat{n}_2 \cos \alpha_2} \tag{3}$$

and

$$r_p = \frac{\hat{n}_1 \cos \alpha_2 - \hat{n}_2 \cos \alpha_1}{\hat{n}_1 \cos \alpha_2 + \hat{n}_2 \cos \alpha_1} \tag{4}$$

where α_1 and α_2 are related to the angle of incidence α_0 by Snell's Law. Note α_0 in this case is the angle relative to a vector normal to the reflecting surface. The reflectivities R_s and R_p are given by: $R_s = |r_s|^2$ and $R_p = |r_p|^2$. Reflectivities R_s and R_p calculated for a single interface between gold and carbon are shown as a function α in Figure 8 and are typical of the soft x-ray spectral region, p polarized light exhibiting strong minima at $\alpha = 45°$, the Brewster angle. Note that the reflectivity is large only for $\alpha \simeq 90°$ (i.e., at near grazing incidence).

In the grazing incidence total external reflection regime, the reflectivity is essentially independent of polarization and can be expressed (after Parratt[38]) as

$$R = \frac{h - (\theta/\theta_c)\sqrt{2}(h-1)^{1/2}}{h + (\theta/\theta_c)\sqrt{2}(h-1)^{1/2}} \tag{5}$$

with

$$h = (\theta/\theta_c)^2 + [[(\theta/\theta_c)^2 - 1]^2 + (\beta/\delta)^2]^{1/2} ,$$

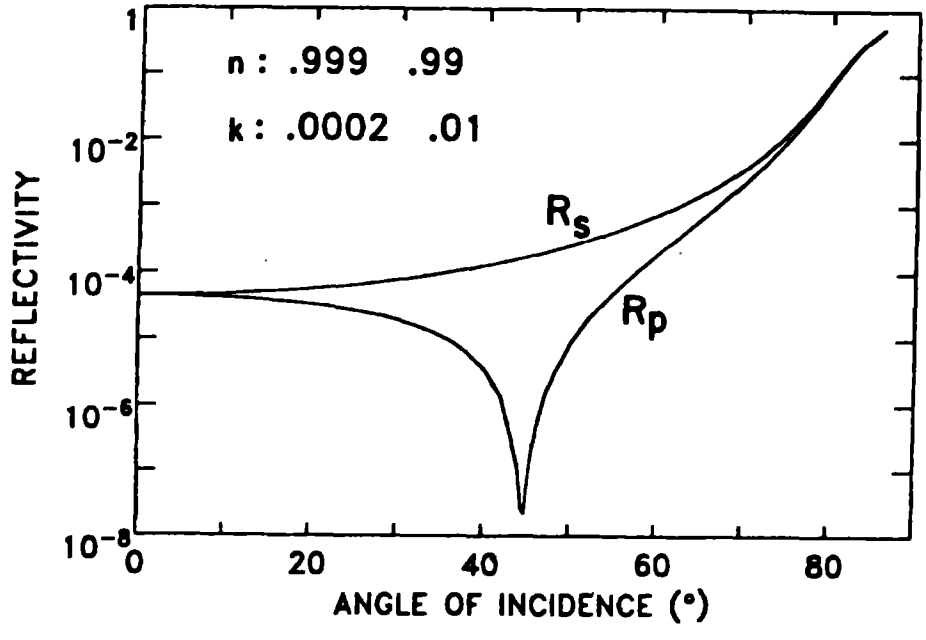

Figure 8. Reflectivities[25] of S and P polarized light at a boundary of carbon and gold plotted as a function of the angle of incidence.

θ the grazing angle of incidence and θ_c the critical angle. The dependence of reflectivity on reduced angle θ/θ_c is shown in The effect of absorption, β, is to decrease the reflectivity in the vicinity of the critical angle. For absorbing scatters, the critical angle is typically taken the value of θ when $R = 0.5$ for β/δ small or the inflection point of the reflectivity curve when β/δ large. An inflection point is not predicted for $\beta/\delta > 0.63$ and a critical angle is not defined for this domain.

An important physical characteristic of the reflection of light in the domain where $\theta \lesssim 0.8\ \theta_c$ is that an evanescent wave[39] exists in the solid so that scattering occurs in some depth. This is seen in the dependence of the reflectivity on the ratio of β/δ in this angular domain as shown in Figure 9. This distance is characterized by a 1/e extinction length, values of which are typically 80 to 100 Å (low density materials) and 20 to 30 Å (high density materials) for x-rays.

X-ray reflectivities of multiple interface structures which include both single films and multilayers on substrates may be calculated by means of a recursion relation using the boundary condition that the tangential components of the light be continuous at the interfaces. For a single layer the reflected amplitudes of the top (r_t) and bottom (r_b) interfaces are calculated using Eq. 3 or Eq. 4. The reflected amplitude of a film is then given as:

$$r = \frac{r_t + r_b\, e^{2i\Delta}}{1 + r_t\, r_b\, e^{2i\Delta}} \tag{6}$$

where

$$\Delta = \frac{2\pi d\, \hat{n} \cos\, \alpha}{\lambda}$$

Δ is the phase shift of the wave with propagation angle α through the thickness d of the film. For a multilayer system, the reflectivity is calculated by recursive application of Eq. 6, successively calculating the reflectivity for each layer using the results of the preceding calculation for one interface in this two interface case until the multilayer is fully traversed. This method fully accounts for dynamical effects and absorption.

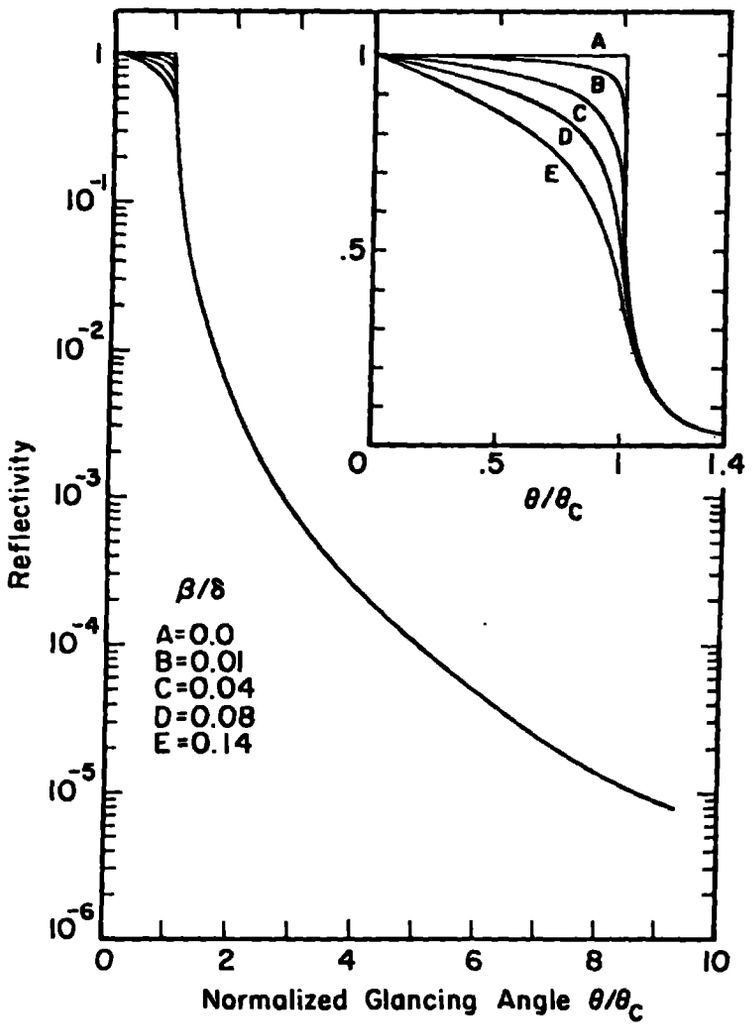

Figure 9. Calculated[59] specular reflectivity of an ideal surface as a function of the reduced glancing angle θ/θ_c for selected values of β/δ.

Several computational approaches of this type[38,40,41,42] have been reported which were specifically designed for x-ray scattering by multilayer structures. Though this approach has only been recently used in this area, it has a long history in modeling normal optics. It can be extended so that the phase and intensity of the x-rays may be calculated at any position in the multilayer under the assumption of an incident plane wave as well as for the reflected light in front of and the transmitted light behind such structures.

Other modeling approaches have been taken which use a scattering formalism. These include the development of a modified Darwin-Prins model for multilayers,[43] a Fresnel zone construction scattering approach[17] (ignoring absorption) for neutron scattering by multilayers, and one[44] following the Ewald-von Laue dynamical theory of crystal diffraction which is directly analogous to the Fresnel approach. Additional approaches are being developed which may be computationally more efficient and allow detailed study of structural effects in multilayers.

The general results of these models are in agreement with diffraction theory for crystal lattices if the multilayers are treated as superlattices with period d equal to the sum of the thicknesses of the two component layers, t_a and t_b. In qualitative terms, the amplitudes of the maxima in reflectivity are directly proportional to the coefficients of the Fourier transform of the electron density distribution introduced by the layering, ignoring absorption. The angular positions, θ_B, of the maxima in reflectivity of light of wavelength λ are given by the Bragg equation 2:

$$m\lambda = 2d \sin \theta_B \qquad (7)$$

where m is the order of reflection. At the Bragg angles, θ_B, the waves scattered by each layer are in phase and the amplitudes add, and intensity is maximum. This equation does not include the effects of refraction or absorption on the Bragg angle θ_B. These are included in the Fresnel calculations but must be added as correction factors for the x-ray scattering case.

The relative magnitudes of these two factors have been calculated by Rosenbluth and Forsyth.[44] They showed that both factors increase the observed

Bragg angle relative to the value calculated using Eq. 7 with the refraction correction dominating except in the vicinity of characteristic absorption edges of the component elements in the soft x-ray domain. The Bragg equation corrected for refraction[2] is

$$m\lambda = 2d \sin \theta_m \left[1 - \frac{2\delta - \delta^2}{\sin^2 \theta_m}\right]^{1/2} \quad (8)$$

where θ_m is the measured Bragg angle. As previously stated, δ is typically of the order of 10^{-5} for x-rays, the correction being therefore important only for small values of θ. When δ is larger, as for soft x-rays or in the EUV, this factor must always be considered.

The Fresnel modeling approaches are currently believed to give accurate results providing the parameters of the sample experimentally studied match those used in the calculations. In the case of an ideal periodic structure, these parameters include the optical constants of the component layers, the thickness of the component layers (A and B) and the number of layers of each. Disagreement between calculation and experiment is typically ascribed to uncertainty in the values of the optical constants or the layer thicknesses. The optical constants are a function of layer composition and density so that these factors underlie any uncertainty in the correct optical constants for a particular atomic specie.

Reported calculations[25,41,42,44,45] for such ideal structures have been specifically directed to prediction of optimized reflectivity over the spectral range of 1 to 124 Å. These calculations have been greatly facilitated by the recent compilation of the optical constants of the elements over the spectral range 6 to 124 Å by B. Henke et al.[46] which have been used by Rosenbluth[47] to calculate optimized normal incidence reflectivities in this spectral range as a function of the component elements and the layer thicknesses. The general result of these calculations is that reflectivities greater than 40% are expected given ideal structures are attainable and the optic constants are

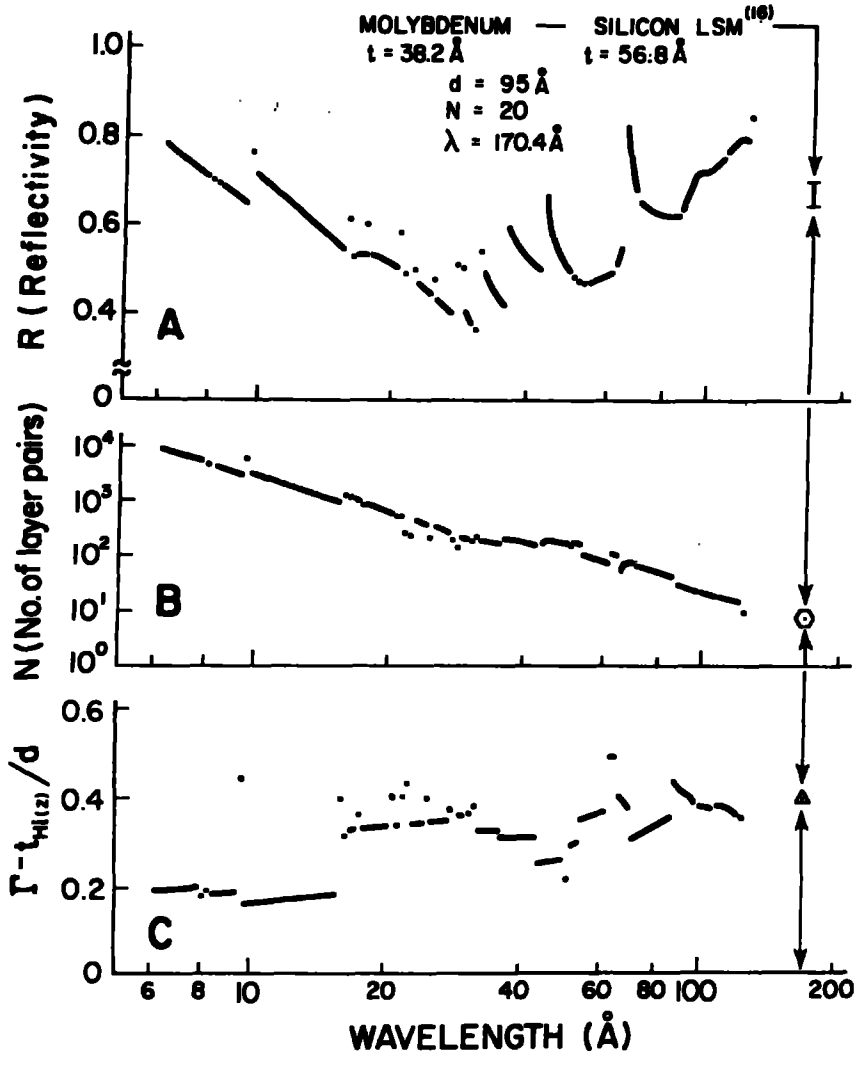

Figure 10. Calculated optimum normal incidence peak reflectivity (R), the number of layer pairs (N) necessary to achieve R, and Γ, the ratio of the thickness of the Hi(Z) scattering layer to the LSM period are plotted as a function of diffracted light wavelength (6.2 Å $\leq \lambda \leq$ 124 Å). These calculations were performed by A. Rosenbluth[47] who used the optical constants reported by Henke, et al.[46] for photon energies of 100 eV $\leq$ E $\leq$ 2000 eV.

correct. These results are shown in Figure 10 where the normal incidence reflectivity (R), the ratio Γ of the thickness of the scattering layer to the multilayer periodicity necessary to attain R and the number of layer pairs necessary are plotted as a function of the reflected light wavelength. These results are in accord with the earlier proposals of Spiller[4] and the modeling results of Vinogradov and Zeldovich.[45]

The important result in this work is that an optimum value of Γ exists for maximum reflectivity which is determined by the optical constants of the constituents. Reflectivity values attainable with periodic structures so optimized are nearly equal to those attainable using aperiodic structures optimized to minimize absorption losses and to maximize phase matching. Also, the bandpasses of multilayer structures are large being 100 to 1000 times those of normal high resolution crystals.

Ideal samples have not been synthesized at this point though excellent results have been achieved in many cases. Several types of "imperfections" are postulated for all the structures listed at the beginning of this section. These include: interfacial (surface) or substrate roughness, long wavelength slope errors of the substrate relative to a mean surface plane, in depth density fluctuations at substrate surfaces, uncertainty in the optical constants for the component elemental species, random errors in thicknesses of deposited layers, compositionally graded interfaces in multilayers, compositional uncertainties for layers in multilayers, and unknown densities for component layers in multilayers. Many of these can be experimentally determined by independent means, though several are inferred, by analysis of reflectivity data using specific models, parameters intended to characterize a particular imperfection being varied to give best fit. This has generally been the case for interfacial (substrate) roughness,[25,28B,48,49] in depth density fluctuations at the surfaces of substrates[50] and compositionally graded interfaces.[41,51]

Many models of surface roughness scattering effects[35,36,37,50] for substrates or single layers on substrates have been developed and compared to experiment. Experiment in this case includes both specular and non-specular reflectivity measurements and independent measurements of surface roughness. This imperfection is crucial to imaging applications, at least at grazing incidence, as non-specular scattering disburses the x-ray beam over an angular

range about the specular beam degrading resolution. Roughness is expected to also degrade resolution in multilayer imaging systems. One model[35,36] treats surface roughness by assuming that the surface acts as a distributed diffraction grating, the periods of which are a function of the surface topography. Another[37] assumes that surface roughness may be represented by an isotropic surface consisting of facets parallel to the mean surface plane located at a distribution of distances from that plane and having a distribution of sizes and shapes. In both approaches, Gaussian distributions are assumed for the parameters characterizing the surface topography. The diffraction grating model has been used extensively for analysis of experimental data in the grazing incidence x-ray domain and will be discussed further here. The facet models, though not as widely applied, have recently been successfully used[52] to study the effects of surface topography on the normal incidence reflectivity $Cd_3 As_2$ for wavelengths above 2000 Å, explaining anomalies in optical constants derived from such data. Matsushita et al.[53] have also reported x-ray glancing angle results which demonstrate that surface faceting must be included in any modeling, though the nature of an appropriate model is not clear.

A general conclusion of all the theories is the prediction of the ratios of both the specularly (I_s) and non-specularly (I_{ns}) scattered intensities from a rough surface to the specularly scattered intensity (I_T) predicted for a perfect surface of the same material. These ratios are called Total Integrated Scatter (TIS) and are

$$I_s/I_T = \exp\left(-\left[4\pi \frac{\cos \alpha}{\lambda} \langle\sigma\rangle\right]^2\right) \tag{9}$$

and

$$I_{ns}/I_T = 1 - \exp\left(-\left[4\pi \frac{\cos \alpha}{\lambda} \langle\sigma\rangle\right]^2\right) \tag{10}$$

where α is the angle measured from the surface normal and $\langle\sigma\rangle$ a parameter characterizing the rms micro-roughness of the surface. Limitations of these theories are that they assume a function $Z(X,Y)$ describing the geometry of the surface which is Gaussian, they apply in the smooth surface limit ($I_s/I_T \simeq 1$) and that slope variations relative to a mean surface plane must be small.

In general, the surface topography is represented by a power spectral distribution which is a function of the two-dimensional surface profile $Z(X,Y)$. It is postulated that scattering into a non-specular direction results from diffraction by a single spatial wavelength component of period d_s on the surface via the grating equation:[3]

$$\lambda = d_s |\cos \theta_s - \cos \theta_i| \tag{11}$$

where θ_i and θ_s are the grazing angles of incidence and scatter respectively. The model surface therefore scatters as if it were a superposition of a sinusoidal gratings of varying amplitude and period. The TIS is then related to the amplitude distribution of the spatial wavelength on the surface through $\langle\sigma\rangle$.

As previously mentioned, correlation of the x-ray TIS data with independent surface characterization is now being actively pursued. This is implemented by measurement of I_{ns} as a function of angle relative to a fixed glancing angle of specular scattering $\theta(I_s)$, and characterization of the surface topography by visible light scattering, mechanical probes, electron microscopy, and interferometry as well as other means. Difficulties in these correlations arising from the limitations of the independent characterization techniques relative to the large bandwidth of surface wavelengths which must be characterized have been discussed by Church et al.[54] Irrespective of these difficulties, Zombeck et al.[55] have compared measurements on very high quality metal coated surfaces with theory and derived $\langle\sigma\rangle$ values in agreement with independently determined data. This model has also been successfully applied[56,57] to evaluation of scattering from polished zerodur flats and Kannigen surfaces with $\langle\sigma\rangle$ values of 3 to 120 Å respectively. This diffractive approach appears, therefore, to effectively model the effects of surface micro-roughness for fixed angles of incidence less than approximately $0.75\ \theta/\theta_c$ for both uncoated and coated surfaces.

If the specular reflectivity, I_s, is measured at a fixed wavelength as a function of the angle of incidence for $0 < \theta/\theta_c < 4.0$ or at a fixed angle of incidence with a white x-ray beam so that same broad range in reduced angle is

spanned by the bandwidth of the incident x-ray beam, the agreement between TIS modeling for I_s and experiment is not good. Good agreement is attainable with a graded index Fresnel model proposed by Nevot and Croce[50] and commented upon and used by A.G. Turyanskii and K.V. Kiseleve[58] and D.H. Bilderback[59] for a variety of surfaces. In this model, the index is assumed equal to 1 at the surface and to vary with depth according to the error function to the value appropriate for the bulk material. Multiple interface structures may be also modeled in this fashion.

The effects of interfacial roughness in multilayer structures have been treated by a number of approaches including the two described: TIS and graded interfaces. First, the TIS formulation (Eq. 9) has been used as a simple multiplier for the reflectivity predicted for an ideal structure. This assumes that the effects of interfacial roughness are non-interacting interface to interface, and tha the structure of a given interface is independent of the structures of other interfaces. Though this approach is phenominological, its convenience is useful. In the graded interface case, all interfaces of the same type (A to B or B to A) are assumed identical, the gradient parameters adjusted for best fit. These two approaches are, in a theoretical sense, in the limit of identical films.

The effects of two kinds of non-identical roughness have been modeled by Rosenbluth and Forsyth.[44] They assume the roughness profiles of different layers are uncorrelated and that they may be described as "roughening" or "smoothing." In roughening films, the roughness of a given film is added to the roughness resulting from preceding layers. Therefore, the absolute roughness of the top layers increases in a random walk fashion as more layers are added. This means that the loss of phase matching over any area of the surface due to roughness induced thickness variations increases as the multilayer is built. The reflectivities of roughening films are very sensitive to roughness falling rapidly to zero for $\langle\sigma\rangle$ values less than 1 Å for a tungsten-carbon structure (d = 36.1Å) containing 250 layer pairs reflecting 67.6 Å light at normal incidence. In "smoothening" films, the roughness is assumed to be self-compensating so that although the roughness of a single interface may be large, the effects of this roughness are compensated for by other layers. Calculations indicate that smoothening films result in reflectivities approaching those

predicted for identical films at the same value of roughness. These authors state that the effects of smoothening film roughness are similar to those of graded index interfaces when the roughness is small.

In this section, a short review of pertinent theory has been presented. The most highly developed models available are for uncoated or coated single surface scattering. Multilayer scattering has been well treated using ideal structure models with modeling for the effects of imperfections at an early stage.

MULTILAYERS ON FIGURED SURFACES

The properties of interest for such composite structures are the reflectivity and optic quality of the reflected light. It is clear from the preceding discussions that both these are complex functions of the atomic and near atomic structure of substrate surfaces and multilayers, and depend on the optic constants of the elemental constituents of the multilayer. At this time, the majority of the multilayer experimental work has been directed to the understanding of synthesis process-multilayer performance relationships, characterization of multilayer reflectivities over a range of wavelengths, synthesis and characterization of unique multilayer structures such as Fabry-Perot etalons[60,61,62] and depth and length graded period[63,64] structures, and selected applications. Almost all of this work has been performed using flat substrates and then, almost all the flat substrates have been commercial device quality single crystal (111) orientation silicon wafers. Only a limited number of experimental studies of multilayers deposited on prepared flat or figured surfaces have been reported. Therefore, this discussion of the experimental status of x-ray optics using multilayers on figured substrates will also review the current status of multilayer development drawing, on theory when possible. A discussion of experimental results for single layers is given first as this work is of direct interest.

SINGLE LAYERS

A short discussion of interference measurement of thin film roughness during synthesis was given in the Multilayer Synthesis section. This approach

has been applied[25,26] in a number of laboratories to an extensive list of materials. In one case[65] the same samples were studied by scanning electron microscopy as an independent measure of surface roughness. Results obtained by these two methods correlated well. Also, results obtained in different laboratories for the same materials by the x-ray technique are in agreement. Since these results are for thin films deposited on substrates, the substrate roughness is accounted for by assuming the two roughness components add in Gaussian quadrature. Derived $\langle\sigma\rangle$ values for a number of 100 Å thick elemental and alloy films are given in Table 1. Substrates and substrate roughness (when available) values are also listed. Those materials exhibiting the smallest roughness or smoothening are of most interest for multilayer structures.

These results are encouraging since they demonstrate that films with near atomic roughness in an x-ray sense may be synthecized. Additionally, WRe and C films, which are amorphous, exhibit the lowest roughness levels, as expected. Although crystalline flat atomically smooth surfaces represent the ideal limit for smooth surfaces, amorphous films are expected to have roughnesses of the order of an atomic diameter or less. This indicates that amorphous films will be very useful for longer period multilayers though thin single crystal films for small period ($d \leq 15$ Å) structures are likely to be necessary.

MULTILAYER REFLECTIVITY

Reflectivities have been determined over the spectral range 0.6 to 200 Å for multilayer samples on flat substrates at fixed angles of incidence as a function of the wavelength of the incident light and at fixed wavelength as a function of the angle of incidence. Two specific types of measurements are made: absolute reflectivity and integrated reflectivity. In the x-ray wavelength domain absolute measurements can be made using laboratory sources[26,28B,33,48,49,50,51,59,60,62] and at synchrotron facilities.[28B,66,67] In the soft x-ray domain integrated reflectivities are typically measured with laboratory sources[11,68] and absolute reflectivities using synchrotron facilities.[24,51,62,69,70,71,72,73] Absolute reflectivities have been measured using both laboratory[74] and synchrotron

sources[69,71,75,76,77] in the EUV. These measurements have been primarily directed to determination of reflectivities for comparison with calculated values.

Three types of comparison are typically made: First, the peak reflectivities in the orders of reflection measured are compared with theory; second, the integrated reflectivities are compared with theory; third, the full reflectivity curves are compared with theory. As might be expected the last of these is most informative although the first two demonstrate the quality of the multilayer structure studied. Several conclusions have been reached as a result of these experimental studies. First, in all cases where reasonable certainty for the values of the optical constants used in the modelling calculations exist, the observed reflectivities are smaller than expected. This appears to be the case for wavelengths up to 124 Å. Uncertainty in the optical constants at longer wavelengths in the EUV leads to the use of calculation more as a guide than for absolute comparison. Second, in almost all cases the bandpass or resolution of observed Bragg reflections are in agreement with calculation. This suggests that the structures are highly periodic though the reduced reflectivities might result from the random errors in the periodicity of the multilayer. This conclusion is unverified and requires experimental support before it can be more than an inference. Third, reflectivities measured in the x-ray domain are in better agreement with calculation than those measured in the soft x-ray or EUV spectral domains. This is now believed the result of structural imperfections whose effects are a function of photon wavelength, more strongly affecting longer wavelength reflectivities. X-ray reflectivities for multilayers synthecized from a well-characterized material pair are typically 85 to 90% of prediction. This value falls to 50 to 60% in the soft x-ray domain.

Recent experimental[73] results for periodic multilayers of cobalt, iron or nickel layered with carbon have shown substantially improved results as illustrated in Figure 11. The observed reflectivities are 78% (215 eV) and 71% (246 eV) of calculation. The quoted layer thicknesses for cobalt in this sample are 14.6 Å which is 7.1 times the (111) plane spacing in FCC cobalt. The carbon in the multilayer is amorphous and smooth. This excess 0.1 atomic planes of cobalt may act as roughness or as a random error in the period of this multilayer depending on the in plane correlation length of the resulting atomic

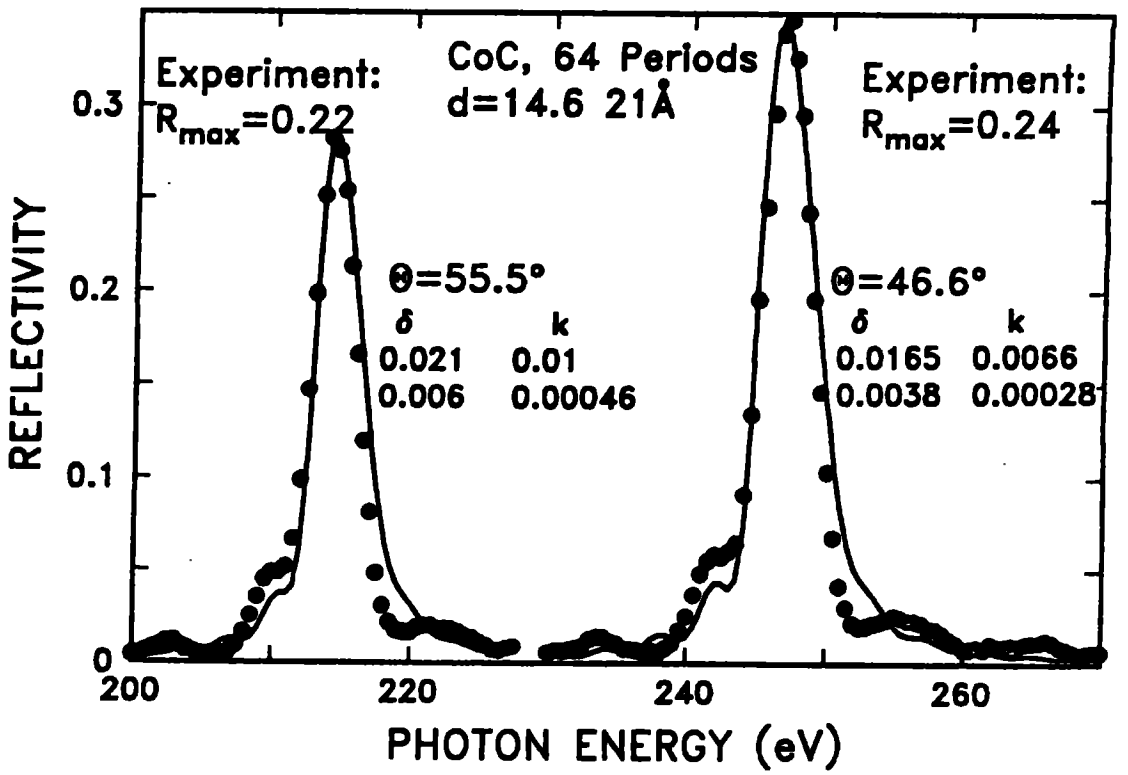

Figure 11. Measured and theoretical (solid line) reflectivities[73] of a Co-C multilayer (d = 35.6 Å, t_{Co} = 14.1 Å) containing 128 layers at two angles of incidence.

steps. It is likely that perfection at this level results in the excellent quality of this sample. This interpretation agrees with the results of Flevaris et al.[27] for Ni-Cu multilayers discussed earlier.

A recent study[74] in the EUV of molybdenum-silicon multilayers yielded reflectivities equal to or larger than those calculated. A comparison of the observed reflectivity of 170.4 Å radiation and model calculations is shown in Figure 12 as a function of angle, ϕ, relative to normal incidence. The angular position of the reflection and its form agree with calculation, but the experimental reflectivity is 1.5 times the calculated value. This may be rationalized as resulting from an over-estimate of the adsorption co-efficients by approximately 35%, a value well within the scatter of values reported in literature. Reflectivities for 8 keV x-rays were also measured. Efficiency in first order was ~ 85% and Bragg peaks were observed through 16th order. In this sample the molybdenum layers were 17.1 times the (110) plane spacing in BCC molybdenum. Also the effective periodicity in 16th order for this multilayer is approximately 6 Å which indicates that the interfaces are uniform to at least this level.

Absolute reflectivity measurements at near normal incidence in the EUV on molybdenum-silicon structures deposited onto 1 meter and 2 meter radius spherically ground superpolished quartz substrates have recently been made by Keski Kuhla.[77] S polarization reflectivities at 15 and 20° off normal for 170 to 190 Å light were in the range 42 to 47%. This is comparable to may samples deposited on flat silicon substrates but substantially less than the maximum values previously observed. These results are highly encouraging, demonstrating that reflectivities from multilayers on truly figured surfaces can be as large as from those on flats. Gaponov et al[69] also observed EUV reflectivities from concave spherial multilayer mirrors which correlated well with flat sample results and had optic quality better than the apparatus could measure.

These results are very significant to the field. They imply that if sufficiently high multilayer quality is achieved, reflectivities as calculated by Rosenbluth (see Figure 10) may be realized. It is also likely that the increased agreement between experiment and calculation shown for the cobalt-carbon sample verifies the optical constant results reported by Henke et al.[46]

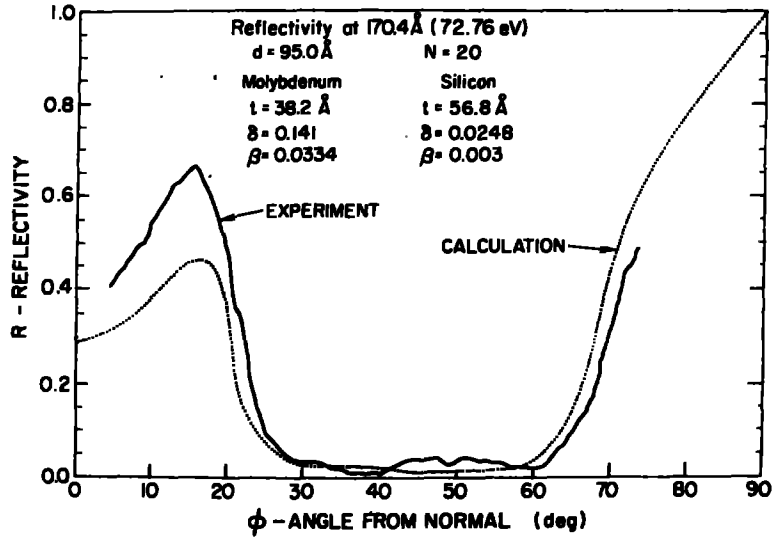

Figure 12. Experimentally observed reflectivity[74] of 170.4 Å light by a molybdenum-silicon multilayer containing twenty layer pairs (Mo-Si) is shown and compared to model calculations made using the optical constants given.

It is important to note the general explanations which have been put forward to explain the disagreement between experimental and theoretical reflectivities. The first is that the optical constants used in the calculations do not correspond to those of the actual layers in the multilayers. An experiment[66] in which a titanium-carbon sample was used to determine the scattering anomalous dispersion co-efficient of titanium by analysis of reflectivity measurements at energies spanning the Ti K absorption edge has been reported. The titanium layers in this sample were 26.4 Å thick. The results obtained were in excellent agreement with values[78] determined by transformation of transmission adsorption data by means of the Kramers-Kronig relationships. Therefore, in this case the optical constants of the titanium in this multilayer are those of bulk titanium.

A similar, but not as quantitative, conclusion[28B] was reached through analysis of refraction caused shifts in the angular positions of first order Bragg peakss of a vanadium-carbon multilayer over the energy range 108 eV to 13000 eV. In this case comparison was with the optical constants reported by Henke et al.[46] The experimental values of δ for the multilayer were generally within 10 to 15% of the calculated values, except near the absorption edge of carbon at 277 eV. This agreement is considered quite reasonable considering the simplicity of the analysis used.

The second imperfection is random thickness errors in the periodicity of the multilayers. Rosenbluth and Forsyth[44] calculated that such errors will result in a decrease in the reflectivity and an increase in the bandwidths of the multilayer reflections. Model calculations by McWhan et al.[79] using atomic diffraction theory indicate that the reflectivity should be decreased but that the bandwidth should be unchanged. This later result is in agreement[80] with thermal effects in normal crystal lattices and is termed the Debye-Waller effect. In the crystal lattice case diffuse scattering[80] in regions away from the Bragg peaks is increased by thermal effects. This should also be seen in multilayer structures. In any case, it should be expected that multilayer scattering will be directly analogous to crystal lattice scattering if the errors in periodicity are random, not too large a magnitude, and the number of layers participating in the reflection process is relatively large.

The third approach invokes interface imperfection which can be either composition gradients or interfacial roughness. The graded interface approach allows fitting of the reflectivity curves[50,51] for x-rays over a broad angular range through many orders. The composition or refractive index gradients at the interfaces are treated as fitting parameters. As noted earlier Rosenbluth's model indicates that interfacial roughness in the smoothening film case is equivalent to graded interfaces at small amplitudes. The interfacial roughness approach has typically used the TIS formalism as expressed in Equation 9. This, by means of the Bragg equation (Eq. 7) may be written as:

$$I_s/I_T = \exp[-(2\pi m \frac{\langle\sigma\rangle}{d})^2] \qquad (12)$$

where m is the order of the reflection and d the period. Equations 9 and 12 have been used to infer interfacial roughness in accord with the results for 100 Å films (see Table 1) giving some support to this approach. Additionally Eq. 12 has been applied to a vanadium carbon multilayer,[28B] adequately explaining the differences between experiment and calculation for the first four orders of reflection for photon energies of 5300 eV and 6000 eV by an interfacial roughness of 7.7 ± 0.5 Å.

Another series of experiments[28B] in which the reflectivity in first order for a series of tungsten-carbon multilayers with periods ranging from 5 to 52 Å that were designed to have the same reflectivity have been reported. The reflectivity for 8 keV x-rays decreased in a manner fit reasonably well by Eq. 12, assuming $\langle\sigma\rangle$ = 3.15 Å. The agreement achieved was sufficient to support the hypothesis that interfacial roughness is an important structural parameter.

The major conclusions of this section on Multilayer Reflectivity are:

1) Structural perfection of multilayer structures is a major factor in determining reflectivity.
2) Characterization of the level of perfection by means of more than phenomenological modelling is very limited.
3) The optical constants used in most modeling calculations are probably reasonable values for the multilayer component layers.

4) More detailed studies with samples containing engineered imperfections are needed, if understanding is to be achieved.
5) Multilayers deposited on truly figured surfaced can have high reflectivity.
6) Effects of substrate roughness have not been systematically investigated.

OPTIC QUALITY

Multilayer x-ray optics applications will in general require high optic quality. Optic quality requires that the optic not introduce unwanted intensity variations into the specular scattered beam and not degrade the rectilinear propagation of the beam through the optic. Such applications include two surface monochrommators, x-ray microscopes, x-ray microprobes, high flux insertion device optics, and any applications in which focussing is required.

To my knowledge only one normal incidence focussing multilayer optic imaging experiment[81] has been reported. A tungsten-carbon multilayer deposited onto a flat (111) silicon substrate was used. This substrate was four point loaded around its circumference so that a concave spherical mirror was approximated. An image of a grid was taken with 277 eV light, resolution being at the 50 to 100 μ scale. This resolution was limited by surface quality of the silicon substrate, the x-ray source, and the optic quality of the bending figure.

The optic quality of multilayer elements has been investigated in four reported studies which have demonstrated that the primary error is substrate figure quality. J.P. Henry et al.[82] have tested an multilayer normal incidence astronomical telescope mirror reporting an angular resolution of better than 1 arc sec. They indicate this resolution was limited by the spatial resolution of the detector and by geometrical constraints in the test equipment. More recently D.H. Bilderback et al.[67] tested the optic quality of LSM's deposited onto commercial single crystal silicon wafer surfaces and of as received substrates, concluding that substrate defects resulting from surface slope errors > 10 arc sec's were the limiting optic defect. There was no evidence in this work that the LSM's degraded the optic quality of the incident light beam. This indicates that LSM coatings mimic the undulations of the substrate so that substrate quality must be excellent for applications requiring high optic performance.

A similar conclusion is reached by Warburton et al.[83,84] In these experiments diffracted beam monochromators [Si (220)] having a measured 4.05 sec F.W.H.M. ($E/\Delta E \simeq 1.0 \times 10^4$) at 8 keV were used. It was possible, with this experimental arrangement, coupled to either a scatter slit with white light incident or to an incident light monochromator, to demonstrate that substrate defects are limiting LSM performance and that non-specular multilayer caused scattering appears to be small.

This has been further demonstrated[85] with LSMs deposited onto x-ray optic quality flats and onto silicon single crystal substrates. These samples were used as a pre-monochromator crystals to a standard S.S.R.L. two crystal (111) silicon monochromator. EXAFS spectra of nickel were taken with and without the LSM premonochromator. When silicon substrate LSM's were used, the EXAFS resolution was observed to be strongly degraded, this effect being directly attributable to slope errors on the silicon. When the LSM on the x-ray optic flat was used as a premonochromator no degradation of the Ni EXAFS spectra was observed relative to the spectra taken using only the (111) Si monochromator as shown in Figure 13.

This work has shown that the optic quality of substrates is singularly important in determining the optic quality of LSM based reflecting optics. The primary imperfection appears to be slope errors. Evidence at this point indicated that for LSM's having individual layer thicknesses greater than 7 Å, this substrate characteristic will control the LSM behavior for applications requiring high optic quality. It is also possible that substrate quality dominates the response of smaller period LSM's ($d < 15$ Å) since the predicted LSM acceptance angles are approximately 60 arc sec compared to substrate slope errors of greater than 10 arc secs for small surface areas, and considerably larger over extended surface areas.

Substrate roughness effects can degrade the optic quality of light reflected from multilayer structures in a manner directly analogous to coated or uncoated single surfaces. In addition, x-ray topographs[82,86] taken using 8000 eV and 1500 eV light have demonstrated intensity variations in the light reflected by multilayers on silicon surfaces. These intensity fluctuations can result from simple geometric effects or interference of the pencil beams reflected by surface facets at the detector plane. If the facet size is small,

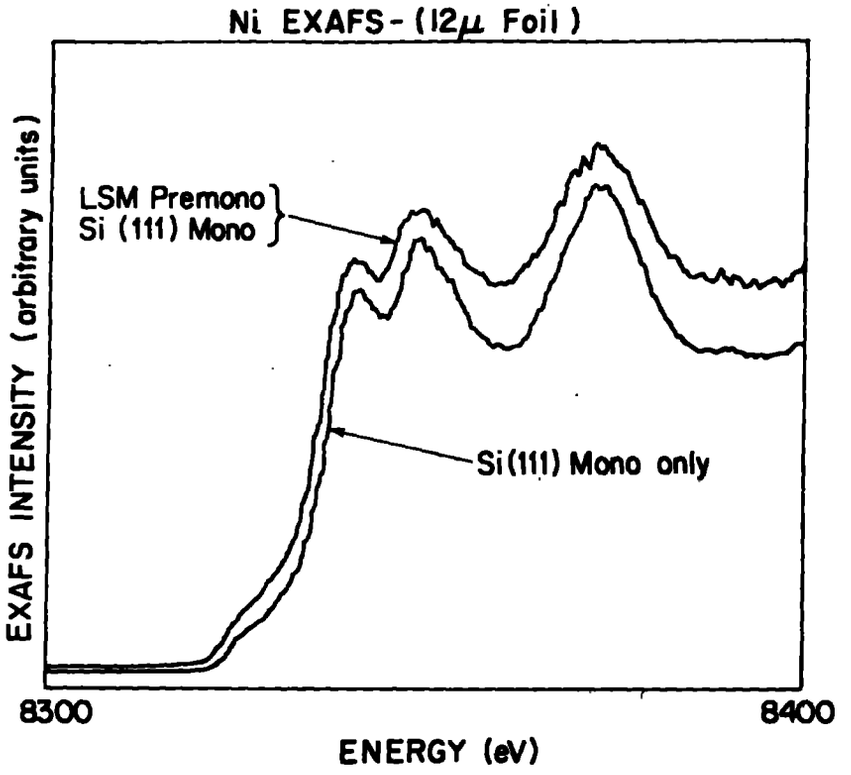

Figure 13. An Extended X-ray Absorption Fine Structure (EXAFS) spectrum of a 12μ thick nickel foil[85] over the energy range 8300 to 8400 eV obtained using a two crystal (111) silicon monochromator is compared to an EXAFS spectrum from the same nickel foil taken using the same two crystal (111) silicon crystal monochromator preceded by a tungsten-carbon LSM premonochromator. The LSM structural parameters are: t_w = 13.2 Å, t_c = 19.8 Å, N(W/C) = 100.

size dependent interference may also occur. These possibilities are directly related to the degree of unflatness of the substrate surface.

Specular scattering results obtained by Matsushita et al.[53] from a number of surfaces demonstrated that facetting or surface slope errors are present even on super polished surfaces. He observed an asymmetry in the intensity of non-specular light scattered about a specular beam, the incident beam striking the surface at the critical angle. Facetting which locally decreases the angle of incidence may cause a substantial enhancement in non-specular scattering. If the local angle of incidence is increased the non-specular scattering is decreased. This is caused by the strong angular dependence in specular scattering at the critical angle. Their results showed that a major portion of the non-specularly scattered light arises from unflatness (facetting and surface slope errors).

DISCUSSION

Two primary conclusions are apparent from the material presented. First, the major points to be understood relative to figured multilayer x-ray optics concern the effects of imperfections in the multilayers and imperfections in the substrates. The second is that only a limited amount of information is available in either of these areas so that significantly more theoretical and experimental work is needed.

It is particularly instructive to examine the effects of surface flatness and roughness in the semi-infinite media case as these form the basis for discussion of the effects of such structural features in multilayers, relative to their reflectivity and the optic quality of the reflected light. The effect of these to topographical characteristics (flatness and roughness) is scattering which results in phase fluctuations in the reflected wavefront by surface height or orientation variations which upset the interference process needed for rectilinear propagation as well as scattering light out of the acceptance angle of any detector.

It is possible, in a semiquantitative sense, to define the scale of two domains in which geometric (flatness) and diffractive (roughness) scattering are dominant. A simple analysis for grazing incidence put forward by Aschenbach[62] is used in the following.

If the surface topography is Fourier transformed the geometric slope error introduced by the jth component of amplitude A_j and spatial wavelength d_j is

$$\phi_j = \frac{2\pi A_j}{d_j} \tag{13}$$

which results in a deflection angle relative to the zero order beam of $2\phi_j$. In the case of diffraction scattering the scattering angle resulting from a spatial wavelength d_D is given by the grating equation:

$$\phi = \frac{\lambda}{d_D \sin \gamma} \tag{14}$$

where γ is the grazing angle of incidence. The imperfection amplitude at which these two angles are equal $(2\phi_j = \phi)$ is:

$$A_j^* = \frac{\lambda}{4\pi \sin \gamma} \tag{15}$$

which is assumed independent of d_D or d_j, the spatial wavelengths. In the case of total external reflection optics this amplitude is defined in terms of the critical angle and is proportional to the inverse of the square root of the density of the scattering material. Therefore, irrespective of the spatial wavelength, when A_j^* has a value greater than $\lambda/(4\pi \sin \gamma)$ geometric effects dominate. This has some interesting implications for multilayer optics.

The Bragg equation (Eq. 7) defines the relationship between λ and $\sin \gamma$ so that:

$$A_j^* = \frac{d_0}{2\pi} \tag{16}$$

where d_0 is the period of the multilayer. Therefore, for larger period multilayers the amplitude, A_j^* of the surface imperfections at which the transition from the diffractive to the geometric regimes occurs, is larger.

If an angular resolution of 1 arc sec is required a maximum acceptable value of A_j/d_j is defined. Geometric scattering is dominant for A_j values larger than given by Eqs. 15 and 16. For a multilayer having a period of 30 Å surface imperfections of amplitude greater than 5 Å will geometrically scatter light irrespective of their spatial period. If the amplitude is less than 5 Å then only spatial wavelengths greater than approximately 100 μ contribute to geometric scattering, smaller spatial wavelength scattering being diffractive. These limits are demanding if geometric (flatness) effects are to be avoided. They do make it possible, though, to model multilayers on a geometric basis. It is interesting that such a model would be directly analogous to models for mosaic crystalline solids in which the angular distribution of small diffracting volumes is important. A significant difference here is that interference between slightly misoriented pencil beams as well as size caused diffraction effects for individual pencil beams reflected from microfacets should be considered.

If these pencil beams can be considered as equivalent to slits which only pass the fraction of the incident light defined by the multilayer reflectivity, they may be discribed[3] by Fraunhofer diffraction in the far field. If the facet is circular with radius a approximately 80% of the reflected energy lies within a circle of radius $0.61\ \lambda/a$ where λ is the wavelength of the reflected light. Therefore it is in principle possible for facets to reduce the apparent reflectivity of a multilayer to 80% its actual value, if only the zeroeth transmitted order is detected. It is interesting to note that this is more likely for longer wavelength incident light. This will also have an effect on the resolution of any imaging reflection x-ray multilayer optic system.

The observation of smoothening films[4] is also interesting and likely important for multilayer synthesis and reflectivity. For the case of multilayer reflectivity it is important to recognize that under the best conditions the deposited layers are of constant thickness and exactly replicate the topography of the substrate. This is schematically illustrated in Figures 14A and 14B where cross-sections of multilayers on flat smooth substrates without (Figure 14A) and with (Figure 14B) interfacial roughness are shown. Interfacial roughness on layer A introduces roughness into the multilayer. If this roughness is uncorrelated layer to layer the lateral spatial roughness scale on

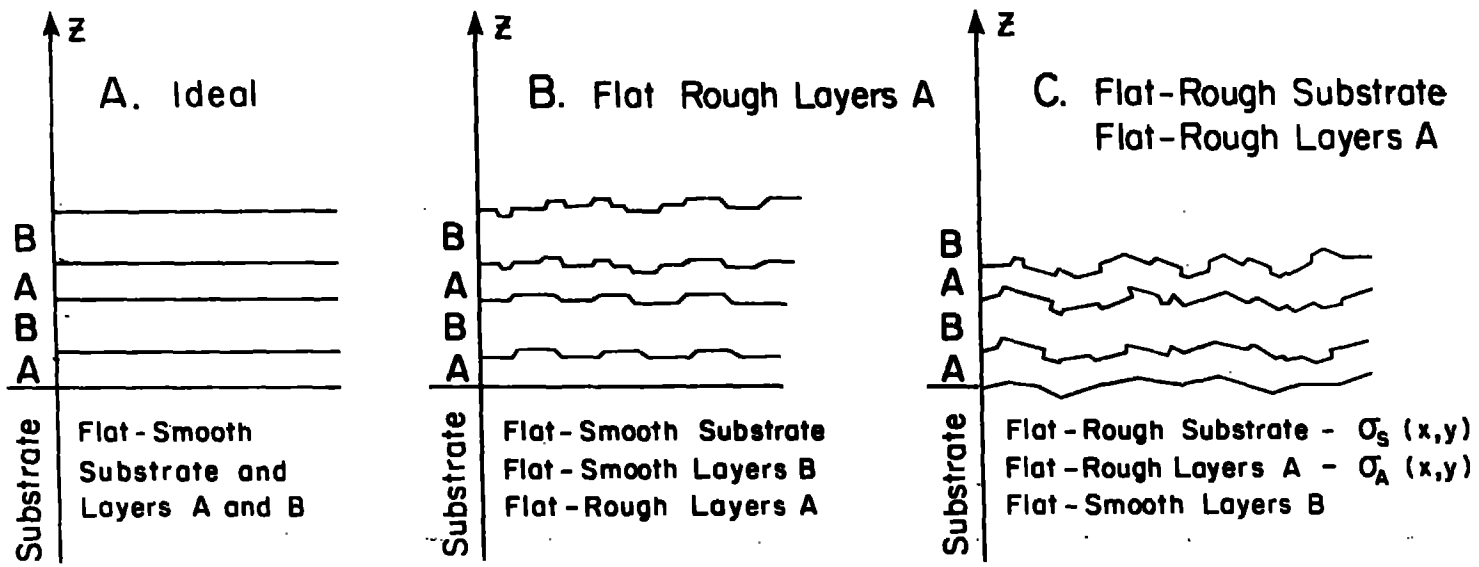

Figure 14. Schematic diagram showing ideal substrate-layer growth (14A), ideal substrate-rough layer growth (14B) and rough substrate-rough layer (14C) growth. If rough-layer growth increases the heterogeneous nucleation site density then "smoothening" is possible.

the nth layer will be substantially smaller than that of a single A layer. A similar result will be observed for substrate roughness as shown in Figure 14C. It is likely that the convolution of the roughnesses of several interfaces will affect subsequent layers inducing either increased roughness or smoothing. If this composite deposition surface roughness strongly affects the nucleation of a subsequently deposited layer it may limit surface roughness by substantially increasing the heterogeneous nucleation site density. The lateral dimension of clusters will be therefore limited and roughness minimized.

CONCLUSIONS

There are many more interesting and exciting subjects in the multilayer x-ray physics field that have not been discussed here. These include the thermal stability of multilayers, multilayers diffraction gratings, geometrically figured substrates for multilayer gratings, multilayer Fabry-Perot etalons, depth graded period multilayers, laterally graded period multilayers, transmission multilayer structures, and many others. All of these will exhibit properties which are strongly affected by the factors considered. In addition, these structures may be applied in unique ways yielding information about the multilayers themselves and thin films deposited on multilayers. It is clear that this field is at an early stage of development so that a wide variety of new and interesting results will be rapidly forthcoming.

ACKNOWLEDGEMENTS

I wish to recognize the continuing support and encouragement of many of my colleagues including D.J. Nagel of the Naval Research Laboratory, John Madey and D.L. Keith of Stanford University, D.T. Attwood of Lawrence Berkeley Laboratories, Pierre Dhez of L.U.R.E., and many others. Preparations of this manuscript was supported by the U.S. Department of Energy through Lawrence Livermore National Laboratory under Contract No. W-7405-Eng-48.

REFERENCES

1. The early work is reviewed by A.H. Compton and S.K. Allison, X-ways in Theory and Experiment, Van Norstrand, New York 1935.
2. James, R.W., The Optical Principles of the Diffraction of X-rays, Oxbow Press, Woodbridge, Conn. 1982.
3. Born, Max and Emil Wolf, Principles of Optics, Pergamon Press, New York 1983.
4. Spiller, E., "Low-Loss Reflection Coatings Using Absorbing Materials," Appl. Phys. Lett., 20, 365 (1972); "Reflective Multilayer Coatings in the Far UV Region," Applied Optics, 15, 2333 (1976); "Multilayer Interference Coatings for the Vacuum Ultraviolet," Proc. ICO-IX, Space Optics, Natl. Acad. Science, Washington (1974) p. 525.
5. Du Mond, J. and J.P. Youtz, "Selective X-ray Diffraction from Artificially Stratified Metal Films Deposited by Evaporation," Phys. Rev., 48, 703 (1935).
6. Du Mond, J. and J.P. Youtz, "An X-ray Method for Determining Rates of Diffusion in the Solid State," J. Appl. Phys., 11, 357 (1940).
7. Dinklage, J. and R. Frerichs, "X-ray Diffraction and Diffusion in Metal Film Layered Structures," J. Appl. Phys., 34, 2633 (1963).
8. Dinklage, J., "X-ray Diffraction by Multilayered Thin Film Structures and Their Diffusion," J. Appl. Phys., 38, 3781 (1967).
9. Blodgett, K.B., "Films Built by Depositing Successive Monomolecular Layers on a Solid Surface," J. Am. Chem. Soc., 57, 1007 (1935).
10. Blodgett, K.B. and I. Langmuir, "Built-Up Films of Barium Stearate and Their Optical Properties," Phys. Rev., 51, 964 (1937).
11. Henke, B.L., "Low Energy X-ray Spectroscopy with Crystals and Multilayers," Low Energy X-ray Diagnostics--1981, (ed. by D.T. Attwood and B.L. Henke), AIP Conf. Proc. No. 75, AIP, New York 1981, p. 85.
12. Dash, J.G. and J. Ruvalds, Phase Transitions in Surface Films, Plenum, New York (1980).
13. Cook, H.E. and J.E. Hilliard, "Interdiffusion in Au-Ag Alloys at Low Temperatures," Appl. Phys. Lett., 8, 24 (1966).

14. Cook, H.E. and J.E. Hilliard, "Effect of Gradient Energy on Diffusion in Gold-Silver Alloys," J. Appl. Phys., 40, 2191 (1969).
15. Cook, H.E., Interdiffussion of Silver-Gold Solutions at Low Temperatures, Ph.D. Thesis, Northwestern University (1967).
16. Schoenborn, B.P., D.L.D. Caspar and O.F. Kammerer, "A Novel Neutron Monochromator," J. Appl. Cryst., 7, 508 (1974).
17. Saxena, A.M. and B.P. Schoenborn, "Multilayer Neutron Monochromators," Acta. Cryst., A33, 805 (1977).
18. Barbee, T.W., Jr. and D.L. Keith, "Synthetic Structures Layered on the Atomic Scale," Workshop on X-ray Instrumentation for Synchrotron Radiation Research, (ed. by H. Winick and G. Brown), Stanford SSRL Report 7804, (1978) III-26.
19. A recent review of both metal and semiconductor super lattice synthesis is contained in L. Chang and B.C. Giessen, Synthetic Modulated Structures, Academic Press (1985).
20. Vossen, J.L. and W. Kern, (ed.) Thin Film Processes, Academic Press, New York (1978).
21. Maissel, L.I. and R. Glang, (ed.) Handbook of Thin Film Technology, McGraw-Hill, New York (1970).
22. Stringfellow, G.B., "Epitaxy," Rep. Prog. Phys., 45, 469 (1982).
23. Wright, J.G., "Electrodeposition," Epitaxial Growth--Part A, (ed. by J.W. Matthews), Academic Press, New York (1975), p. 73.
24. Gaponov, S.V., S.A. Gusev, B.M. Luskin and N. Salashchenko, "Long-Wave X-ray Radiation Mirrors," Opt. Commun., 38, 7 (1981).
25. Spiller, E., "Evaporated Multilayer Dispersion Elements for Soft X-rays," Low Energy X-ray Diagnostic--1981 (ed. D.T. Attwood and B.L. Henke), AIP Conference Proceedings No. 75, AIP, New York, (1981), p. 124.
26. Naccache, D., Realisation de Miroirs Interferentiels X-UV par Controle de Reflectiuitie in Situ, Ph.D. Thesis, L'Universitė Pierre et Marcie Curie, Paris 6 (1983).
27. Flevaris, N.K., D. Baral, J.E. Hilliard and J.B. Ketterson, "A Note on Compositionally Modulated Cu-Ni Films with Lattice-Commsurate Wavelengths," Appl. Phy. Lett. 38, 992 (1981).

28. (A) Barbee, T.W., Jr. and D.L. Keith, "Synthesis of Metastable Materials by Sputter Deposition Techniques," Synthesis and Properties of Metastable Phases (ed. by E.S. Machlin and T.J. Rowland), A.I.M.E., New York (1980), p. 93; (B) Barbee, Troy W., Jr., "Sputtered Layered Synthetic Microstructure (LSM) Dispersion Elements; Layered Synthetic Microstructures (LSM)", Low Energy X-ray Diagnostics 1981, (ed. by D.T. Attwood and B.L. Henke), AIP Conference Proceedings, No. 75, AIP, New York (1981), p. 131; "Reflecting Media for X-ray Optic Elements and Diffracting Structures for the Study of Condensed Matter", Superlattices and Microstructures 1, 311 (1985).
29. Huggins, H.A. and M. Gurvitch, "Magnetron Sputtering System Equipped with a Versatile Substrate Table," J. Vac. Sci. and Tech., A1, 77 (1983).
30. Eltoukhy, A.H., J.L. Zilko, C.E. Wickersham and J.E. Greene, "Compositionally Modulated Sputtered In Sb/GaSb Superlattices; Crystal Growth and Interlayer Diffusion," J. Appl. Phys., 50, 505 (1979).
31. Lamont, L.T., Jr., "Thin Film Symposium, Magnetron Sputtering and Plasma Diagnostics," J. Vac. Sci. and Tech., 15, 171-202 (1978).
32. Namioka, T., Private communication.
33. Zeigler, Eric, Contribution a L'etude de La reflexion des rayons X mous. Conception et realization de multicouches carbone-tungstene, Ph.D. Thesis, Université De Paris--Sud, Centre D'Orsay, (1984).
34. Abeles, B. and T. Tiedje, "Amorphous Semiconductor Superlattices,"Phys Rev. Lett., 51, 2003 (1983).
35. Beckman, P. and A. Spizzichino, The Scattering of Electromagnetic Waves from Rough Surfaces, Pergamon Press, Oxford (1963).
36. Church, E.L., H.A. Jenkinson and J.M. Zavada, "Measurement of the Finish of Diamond-Turned Metal Surfaces by Differential Light Scattering,"; Opt. En., 16, 360 (1977); "Relationship Between Surface Scattering and Microtopographic Features," Opt. Eng. 18, 125 (1979).
37. Porteus, J.O., "Relation Between the Height Distribution of a Rough Surface and the Reflectance at Normal Incidence," J. Opt. Soc. Am., 53, 1384 (1963).
38. Parratt, L.G., "Surface Studies of Solids by Total Reflection of X-rays," Phys. Rev. 95, 359 (1954).

39. Vineyard, G.H., "Grazing-Incidence Diffraetion and the Distorted Wave Approximation for the Study of Surfaces," Phys. Rev. B, 26, 4146 (1982).
40. Segmüller, A., "Observation of X-ray Interferences on Thin Films of Amorphous Silicon," Thin Solid Films, 18, 287 (1973).
41. Underwood, J.H., T.W. Barbee, Jr., and D.L. Keith, "Layered Synthetic Microstructures: Properties and Applications in X-ray Astronomy," Imaging X-ray Optics Workshop, Proc. SPIE 184, 123 (1979); J.H. Underwood, T.W. Barbee, Jr., "Synthetic Multilayers as Gragg Diffractors for X-rays and Extreme Ultraviolet: Calculations and Performance," Low Energy X-ray Diagnostics--1981, (ed. by D.T. Attwood and B.L. Henke) AIP Conf. Proc. No. 75, AIP, New York (1981), p. 170.
42. Lee, P., "X-ray Diffraction in Multilayers," Opt. Commun., 37, 159 (1981); "Application of the WKB Method to X-ray Diffraction by One Dimensional Periodic Structures," Opt. Commun., 42, 195 (1982).
43. Henke, B.L., "Low Energy X-ray Interactions: Photoionization, Scattering, Specular and Bragg Reflection," Low Energy X-ray Diagnostics--1981, (ed. by D.T. Attwood and B.L. Henke), AIP Conf. Proc. No. 75, AIP, New York (1981), p. 146.
44. Rosenbluth, A.E. and J.M. Forsyth, "The Reflecting Properties of Soft X-ray Multilayers," Low Energy X-ray Diagnostics--1981, (ed. by D.T. Attwood and B.L. Henke), AIP Conf. Proc. No. 75, AIP, New York (1981), p. 280.
45. Vinogradov, A.V. and B. Ya. Zeldovich, "X-ray and Far UV Multilayer Mirrors: Principles and Possibilities," Appl. Opt., 16, 89 (1977).
46. Henke, B.L. P. Lee, T.J. Tanaka, R.L. Shimabukuro and B.K. Fujikawa, "Low Energy X-ray Interaction Coefficients: Photoabsorption, Scattering and Reflection. E = 100-2000 eV, Z = 1-94," Atomic and Nuclear Data Table 27 (1982).
47. Rosenbluth, A.E., "Reflecting Properties of X-ray Multilayer Devices," Ph.D. Thesis, University of Rochester (1982).
48. Segmüller, A., "Small-Angle Inteferences of X-rays Reflected From Periodic and Near-Periodic Multilayers," Modulated Structures--1979, (ed. by J.M. Cowley, J.B. Cohen, M.B. Solomon, and B.J. Wuensch), AIP Conf. Proc. No. 53, AIP, New York, (1979), p. 78.

49. Pomerantz, M. and A. Segmuller, "High Resolution X-ray Diffraction From Small Numbers of Langmuir-Blodgett Layers of Manganese Stearate" Thin Solid Films, 68, 33 (1980).

50. Nevot, L. and P. Groce, "Sur l'Etude des Couches Superficielles Monoatomiques par Reflexion 'Rasante' (Speálaire ou Diffuse) de Rayons X, par la Méthode de l'Empilement 'Sandwich'," J. Appl. Cryst., 8, 304 (1975).

51. Dhez, P. "Use of Multilayers for X-UV Optics: Their Fabrication and Tests in France," X-ray Microscopy, (ed. by G. Schmahl and D. Rudolph), Springer-Verlag, New York (1984), p. 139.

52. Jezierski, K. and J. Misiewicz, "Surface Roughness as a Physical Cause of the Dip in the Results of a Kramers-Kronig Analysis of ZN_3P_2," J. Opt. Soc. Am., B1, 850 (1984).

53. Matsushita, T., T. Ishikawa, and K. Kohra, "High Resolution Angle-Resolved X-Rasy Scattering Measurements from Optically Flat Mirrors," KEK Reprint, 82-33, February 1983.

54. Church, E.L., M.R. Howells and T.V. Vorburger, "Spectral Analysis of the Finish of Diamond Turned Mirror Surfaces," Reflecting Optics for Synchrotron Radiation, (ed. by M.R. Howells), Proc. SPIE 315, 202 (1981).

55. Zombeck, M.V., H. Bräuninger, A. Ondrusch and P. Predehl, "High Resolution X-ray Scattering Measurements," High Resolution X-ray Optics, (ed. by E. Spiller), Proc. SPIE 316, 174 (1981).

56. Aschenbach, B. H. Bräuinger, A. Ondrusch and P. Predehl, "X-ray Scattering of Superpolished Flat Mirror Samples," High Resolution Soft X-ray Optics, (ed. by E. Spiller), Proc. SPIE 316, 187 (1981).

57. Aschenbach, B., "The Current Status of Grazing Incidence Optics," New Techniques in X-ray and XUV Optics, (ed. by B.J. Kent and B.E. Patchett), Rutherford Appleton Laboratory, England (1982).

58. Turyanskii, A.G., and K.V. Kiseleva, "Transition-Layer Model in Specular Reflection of X-rays From an Interface Between Two Media," Kratkie Soobshcheniya po Fizike, 8, 20 (1977).

59. Bilderback, D.H., "Reflectance of X-ray Mirrors from 3.8 to 50 keV (3.3 to 0.25°A)," Reflecting Optics for Synchrotron Radiation, (ed. by M.R. Howells), Proc. SPIE 315, 90 (1981).

60. Barbee, T.W., Jr., and J.H. Underwood, "Solid Fabry-Perot Etalons for X-rays," Optics Comm., 48, 161 (1983).
61. Lepetre, Y., R. Rivoria, R. Philip and G. Rasagni, "Fabry-Perot Etalons for X-rays: Construction and Characterization," Optics Comm., 51, 127 (1984).
62. Bartlett, R.J., W.J. Trela, D.R. Kania, T.W. Barbee, Jr., M.P. Hockaday, and P. Lee, "Soft X-ray Measurements of Solid Fabry-Perot Etalons," Optics Comm., 55, 229 (1985).
63. Nagel, D.J., T.W. Barbee, Jr. and J.V. Gilfrich, "Graded-Layer-Thickness Bragg X-ray Reflectors," Reflecting Optics for Synchrotron Radiation, (ed. by M.R. Howells), Proc. SPIE 315, 110 (1981).
64. Barbee, T.W., Jr., "Multilayers for X-ray Optical Applications," X-ray Microscopy, (ed. by G. Schmahl and D. Rudolph), Springer-Verlag, New York, (1984), p. 144.
65. Broers, A.N. and E. Spiller, "A Comparison of High Resolution Scanning Electron Micrographs of Metal Film Coatings with soft X-ray Interference Measurements of Fiulm Roughness," Scanning Electron Microscopy, SEM Inc., AMF O'Hara, (1980), p. 201.
66. Barbee, T.W., Jr., W.K. Warburton, and J.H. Underwood, "Determination of the X-ray Anomalous Dispersion of Titanium Made with a Titanium-Carbon Layered Synthetic Microstructure," J. Opt. Soc. Am., B1, 691 (1984).
67. Bilderbeck, D.H., B.M. Lairson, T.W. Barbee, Jr., G.E. Ice, and C.J. Sparks, "Design of Doubly Focusing, Tunable (5-30 keV), Wide Band Pass Optics Made from Layered Synthetic Microstructures," Nuc. Inst. Meth., 208, 251 (1983).
68. Gilfrich, J.V., D.J. Nagel, and T.W.Barbee, Jr., "Layered Synthetic Microstructures and Dispersing Devices in X-ray Spectrometers," Appl. Spec., 36, 58 (1982).
69. Gaponov, S.V., F.V. Garin, S.L. Guseu, A.V. Kochemasou, Yu. Ya Plantonov and N.N. Salashchenko, "Multilayer Mirrors for Soft X-ray and VUV Radiation," Nuc. Inst. Meth., 208, 227, (1983).
70. Lee, P., R.J. Bartlett and D.R. Kania, "Soft X-ray Optics Using Multilayer Mirrors," Opt. Eng., 24, 197 (1985).
71. Spiller, E., A. Segmüller, J. Rife, and R.-P. Haelbich, "Controlled Fabrication of Multilayer Soft X-ray Mirrors," Appl. Phys. Lett., 37, 1048 (1980).

72. Day, R., J. Grosso, R.J. Bartlett, and Troy W. Barbee, Jr., "Layered Synthetic Microstructures: Measurements and Applications," Nuc. Inst. Meth., 208, 245 (1983).
73. Golub, L., E. Spiller, R.J. Bartlett, M. Hockaday, D.R. Kania, and W.J. Trela, "X-ray Tests of Multilayer Coated Optics," Technical Digest--Third Topical Meeting on Optical Interference Coatings, April 17-19, 1984, Monterey, California, Paper TUA-B3.
74. Barbee, T.W., Jr., S. Mrowka and M.C. Hettrick, "Molybdenum-Silicon Multilayer Mirrors for the Extreme Ultraviolet," Appl. Opt., 24, 883 (1985).
75. Haelbich, R.-P., and C. Kunz, "Multilayer Interference Mirrors for the XUV Range Around 100eV Photon Energy," Opt. Comm., 17, 287 (1976).
76. Haelbich, R.-P., A. Segmüller and E. Spiller, "Smooth Multilayer Films Suitable for X-rays Mirrors," Appl. Phys. Lett., 34, 184 (1979).
77. Keski-Kuha, R., Private communication (1985).
78. Warburton, W.K., K.F. Ludwig, and T.W. Barbee, Jr., "Comparison Between Ti Anomalous X-ray Scattering Factors Obtained from Layered Synthetic Microstructures and the Dispersion Relationship," J. Opt. Soc. Am., B2, 565 (1985).
79. McWhan, D.B., M. Gurvitch, J.M. Rowell, and L.R. Walker, "Structure and Coherence of NbAl Multilayer Films," J. Appl. Phys., 54, 3886 (1983).
80. Azaroff, L.V., R. Kaplow, N. Kato, R.J. Weiss, A.J.C. Wilson and R.A. Young, X-ray Diffraction, McGraw-Hill, New York (1974) p. 101.
81. Underwood, J. and T.W. Barbee, Jr., "Soft X-ray Imaging with a Normal Incidence Mirror," Nature, 294, 429 (1981).
82. Henry, J.P., E. Spiller and M. Weisskopf, "Imaging Performance of a Normal Incidence Soft X-ray Telescope," Appl. Phys. Lett., 40, 25 (1982).
83. Warburton, W.K., Z.U. Rek and T.W. Barbee, Jr., "Performance Tests on Layered Synthetic Microstructures (LSM's) for X-ray Optical Elements," X-ray Microscopy (ed. by G. Schmal and D. Rudolph), Springer-Verlag, New York (1984), p. 163.
84. Warburton, W.K., Z.U. Rek and T.W. Barbee, Jr., "Performance Tests on Layered Synthetic Microstructures (LSMs) for X-ray Optical Applications" submitted for publication.

85. Warburton, W.K., Z.U. Rek and T.W. Barbee, Jr., "High Optic Quality Layered Synthetic Microstructure X-ray Optic Elements" submitted for publication.
86. Pianetta, P., R. Redaelli, T.W. Barbee, Jr., "Performance of Layered Synthetic Microstructures in Monochromatar Applications in the Soft X-ray Region," in Applications of Thin Film Multilayered Structures to X-ray Optics (ed. by G.F. Marshall), Proc. SPIE, Vol, 563, Pg. 393, (1985).

Table 1. Surface roughness on 10 nm thick evaporated films. Substrate material and substrate roughness (when available) are also given.

Thin Film		Substrate		Ref.
Material	Roughness (Å)	Material	Roughness (Å)	
ReW	-3 to +2	float glass	---	25
WRe	0.7 to 4.6	float glass	2.0	26
ReW	0 to 2.5	Si	(4.0)*	25
WRe	0.85 to 4.0	Borosilicate	1.5	26
W	3.0	Si	(4.0)	25
B	1.0	ReW	---	25
B	1.12 to 3.4	float glass	2.0	26
B	1.5 to 3.8	Borosilicate	1.0	26
C	0	ReW	---	25
Si	2.15	float glass	2.6	26
LiF	17.0	ReW	(4.0)	25
Ta	5.2	Si	(4.0)	25
Re	5.2	Si	(4.0)	25
Os	5.3	Si	(4.0)	25
Ir	4.2	Si	(4.0)	25
Pt	2.8 to 6.0	Si; float glass	(4.0); ---	25
PtIr	7.0	Si	(4.0)	25
Au	8.0	Si	(4.0)	25
AuPd	3.3	Si	4.0	25

*This value of $\langle\sigma\rangle$ is that expected for (111) single crystal silicon wafers.

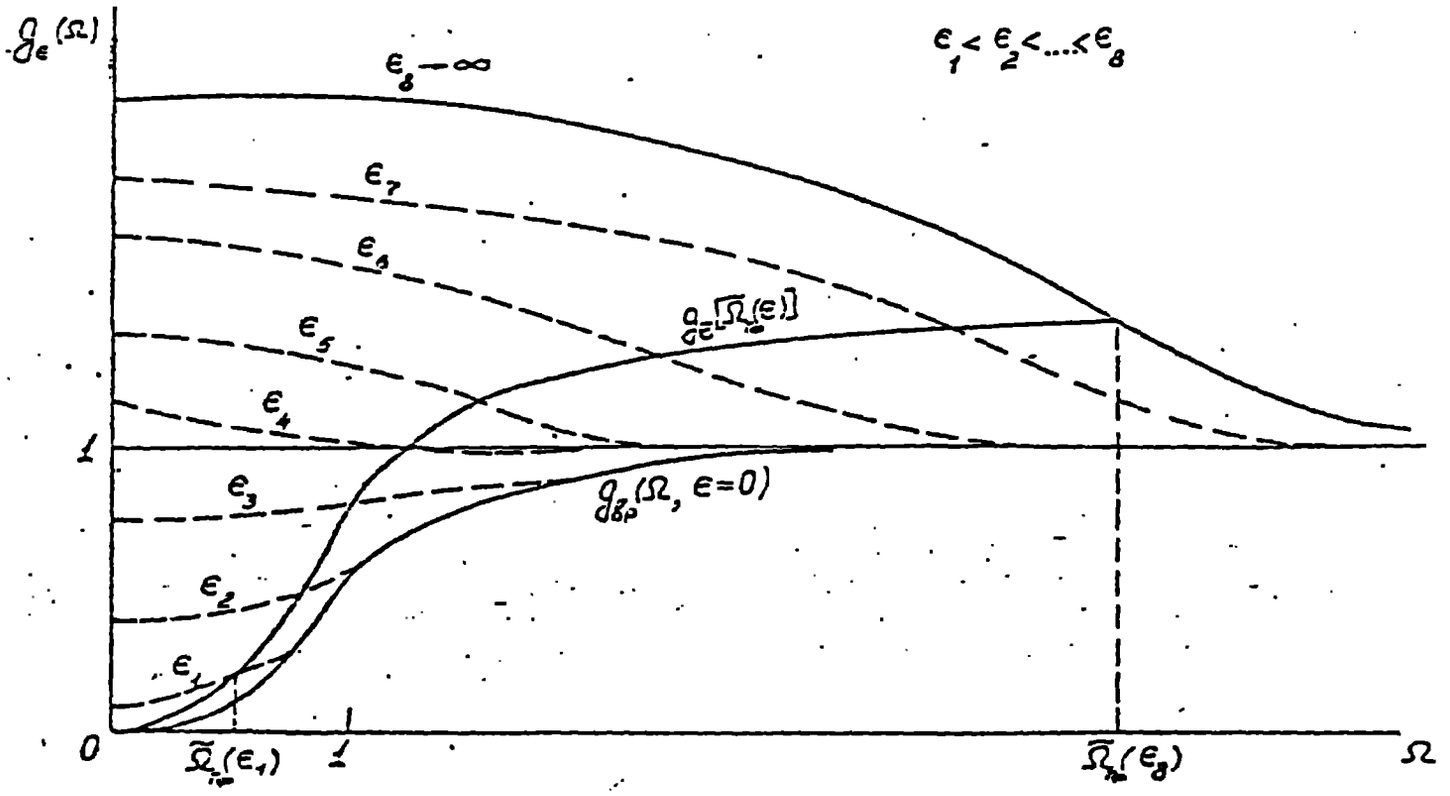

Figure 7. Evolution of classical bremsstrahlung spectra on a neutral atom with a change of parameter ϵ.

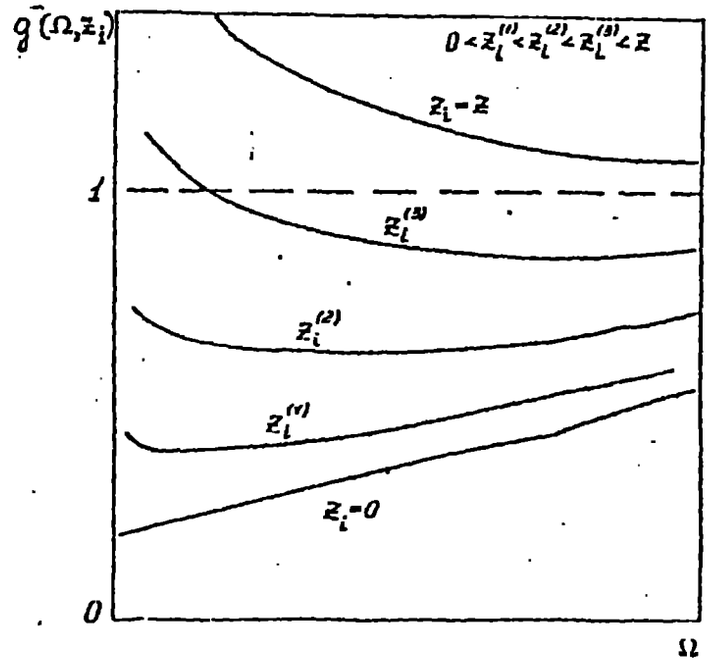

Figure 8. Evolution of classical bremsstrahlung spectrum on an ion in measure with its stripping (Z_i - charge of the ion).

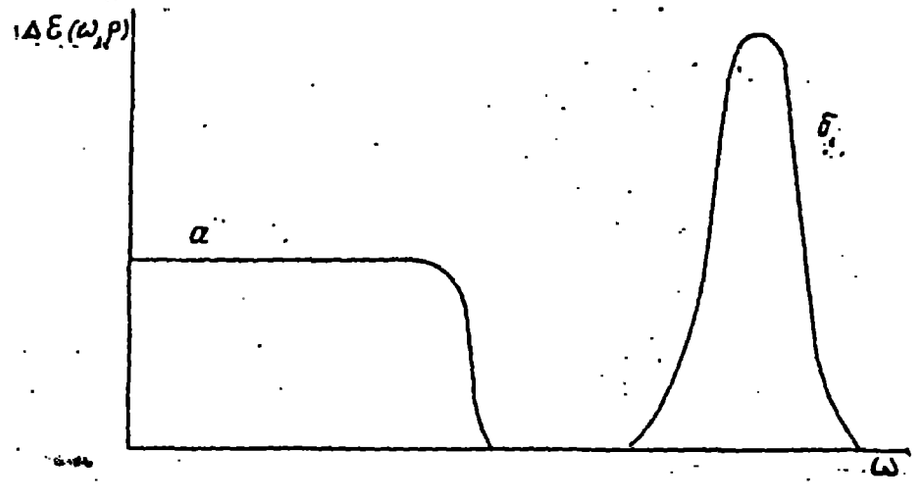

Figure 9. Alternating types of bremsstrahlung of sublines: a - impact; b - pseudostatic.